may reflect evolution of the parasite DHOD to fit the environment present in its mammalian hosts.

The kinetic properties of the three DHODs were comparable, except that DHOD3 had a 2- to 3-fold higher V_{max} and 2-fold higher K_m values for DHO and fumarate. DHOD3 shows replacement of Met2, Leu98, and Arg285 (in DHOD 1 and DHOD2) with Thr2, Val98, and Thr285, respectively. Although these three amino acids are not crucial for catalytic activity, their replacement may lead to alteration of the three-dimensional structure of the protein.

Among DHODs in Tulahuen, the eight amino acids are polymorphic: Met/Thr2, Cys/Arg3, Phe/Val63, Ser/Ile86, Leu/Val98, Leu/Ile222, Thr/Arg285, and Lys/Arg301 (See Fig. 2). Interestingly, all of these amino acid polymorphisms are conserved in the putative DHODs in CL Brener, with two additional polymorphic sites at Gly/Ala223 and Leu/Phe228 [16,17]. Conservation of the amino acid polymorphisms in different *T. cruzi* strains suggests that the amino acid polymorphism in the *DHOD*gene loci have occurred mostly before diversification of *T. cruzi* and conserved during their evolution. It is important that none of the amino acids participating in the catalytic reaction is polymorphic in both Tulahuen and CL Brener. Therefore, it is likely that DHOD isoforms share similar enzymatic properties, despite the extensive nucleotide/amino acid sequence polymorphisms among the gene loci and among *T. cruzi* strains.

Although the *T. cruzi* DHOD gene is highly polymorphic, the gene products are less polymorphic in their kinetic properties. The latter findings are favorable for drug design and facilitate exploitation of drug development. DHOD promises to be a drug target not only for Chagas' disease, but also for malaria, *Pneumocystis carinii* pneumonia, cancers, and autoimmune diseases [20–23]. The DHOD inhibitors currently used and their derivatives should be used to test the three forms of *T. cruzi* DHOD. In addition, marine algae extracts contain a substance that inhibits *T. cruzi* DHOD activity [7]. Crystallographic analyses may determine the precise conformation of *T. cruzi* DHOD, leading to discovery of potent enzyme inhibitors that can be used clinically to treat Chagas' disease.

Acknowledgments

This work was supported in part by grants-in-aid for scientific research (Nos. 15390138, 15659102, 17590377, and 17390123) from the Ministry of Education, Science, Sports, Culture, and Technology of Japan, and from Kampou Science Foundation (to TN). T.AO was supported by a Grant-in-Aid for the 21st Century COE Research from the Ministry of Education, Science, Sports, Culture, and Technology of Japan.

References

[1] Urbina JA, Docampo R. Specific chemotherapy of Chagas disease: controversies and advances. Trends Parasitol 2003;19:495–501.
[2] Urbina JA. Chemotherapy of Chagas disease. Curr Pharm Des 2002; 8:287–95.
[3] Jones ME. Pyrimidine nucleotide biosynthesis in animals: genes, enzymes, and regulation of UMP biosynthesis. Annu Rev Biochem 1980;49:253–79.
[4] Hines V, Keys III LD, Johnston M. Purification and properties of the bovine liver mitochondrial dihydroorotate dehydrogenase. J Biol Chem 1986;261:11386–92.
[5] Takashima E, Inaoka DK, Osanai A, Nara T, Odaka M, Aoki T, et al. Characterization of the dihydroorotate dehydrogenase as a soluble fumarate reductase in *Trypanosoma cruzi*. Mol Biochem Parasitol 2002; 122:189–200.
[6] Nara T, Hashimoto T, Aoki T. Evolutionary implications of the mosaic pyrimidine–biosynthetic pathway in eukaryotes. Gene 2000;257:209–22.
[7] Nara T, Kamei Y, Tsubouchi A, Annoura T, Hirota K, Iizumi K, et al. Inhibitory action of marine algae extracts on the *Trypanosoma cruzi* dihydroorotate dehydrogenase activity and on the protozoan growth in mammalian cells. Parasitol Int 2005;54:59–64.
[8] Gao G, Nara T, Nakajima-Shimada J, Aoki T. Novel organization and sequences of five genes encoding all six enzymes for de novo pyrimidine biosynthesis in *Trypanosoma cruzi*. J Mol Biol 1999;285:149–61.
[9] Nara T, Hirayama-Noguchi Y, Gao G, Murai E, Annoura T, Aoki T. Diversity of aspartate carbamoyltransferase genes of *Trypanosoma cruzi*. Int J Parasitol 2003;33:845–52.
[10] Annoura T, Nara T, Makiuchi T, Hashimoto T, Aoki T. The origin of dihydroorotate dehydrogenase genes of kinetoplastids, with special reference to their biological significance and adaptation to anaerobic, parasitic conditions. J Mol Evol 2005;60:113–27.
[11] Björnberg O, Rowland P, Larsen S, Jensen KF. Active site of dihydroorotate dehydrogenase A from *Lactococcus lactis* investigated by chemical modification and mutagenesis. Biochemistry 1997;36: 16197–205.
[12] Rowland P, Björnberg O, Nielsen FS, Jensen KF, Larsen S. The crystal structure of *Lactococcus lactis* dihydroorotate dehydrogenase A complexed with the enzyme reaction product throws light on its enzymatic function. Protein Sci 1998;7:1269–79.
[13] Rowland P, Nielsen FS, Jensen KF, Larsen S. The crystal structure of the flavin containing enzyme dihydroorotate dehydrogenase A from *Lactococcus lactis*. Structure 1997;5:239–52.
[14] Gutteridge WE, Gaborak M. A re-examination of purine and pyrimidine synthesis in the three main forms of *Trypanosoma cruzi*. Int J Biochem 1979;10:415–22.
[15] Zou CB, Nakajima-Shimada J, Nara T, Aoki T. Cloning and functional expression of Rpn1, a regulatory-particle non-ATPase subunit 1, of proteasome from *Trypanosoma cruzi*. Mol Biochem Parasitol 2000; 110:323–31.
[16] El-Sayed NM, Myler PJ, Bartholomeu DC, Nilsson D, Aggarwal G, Tran AN, et al. The genome sequence of *Trypanosoma cruzi*, etiologic agent of Chagas disease. Science 2005;309:409–15.
[17] http://www.genedb.org/genedb/tcruzi/.
[18] Machado CA, Ayala FJ. Nucleotide sequences provide evidence of genetic exchange among distantly related lineages of *Trypanosoma cruzi*. Proc Natl Acad Sci U S A 2001;98:7396–401.
[19] Atwood III JA, Weatherly DB, Minning TA, Bundy B, Cavola C, Opperdoes FR, et al. The *Trypanosoma cruzi* proteome. Science 2005; 309:473–6.
[20] Ittarat I, Asawamahasakda W, Bartlett MS, Smith JW, Meshnick SR. Effects of atovaquone and other inhibitors on *Pneumocystis carinii* dihydroorotate dehydrogenase. Antimicrob Agents Chemother 1995; 39:325–8.
[21] Chen SF, Ruben RL, Dexter DL. Mechanism of action of the novel anticancer agent 6-fluoro-2-(2′-fluoro-1,1′-biphenyl-4-yl)-3-methyl-4-quinolinecarboxylic acid sodium salt (NSC 368390): inhibition of de novo pyrimidine nucleotide biosynthesis. Cancer Res 1986;46:5014–9.
[22] Baldwin J, Farajallah AM, Malmquist NA, Rathod PK, Phillips MA. Malarial dihydroorotate dehydrogenase. Substrate and inhibitor specificity. J Biol Chem 2002;277:41827–34.
[23] Sanders S, Harisdangkul V. Leflunomide for the treatment of rheumatoid arthritis and autoimmunity. Am J Med Sci 2002;323:190–3.

Available online at www.sciencedirect.com
SCIENCE DIRECT®
Biochimica et Biophysica Acta 1758 (2006) 738–746
BIOCHIMICA ET BIOPHYSICA ACTA
BBA
http://www.elsevier.com/locate/bba

Molecular cloning and characterization of ouabain-insensitive Na^+-ATPase in the parasitic protist, *Trypanosoma cruzi*

Kyoichi Iizumi [a], Yuko Mikami [a,b], Muneaki Hashimoto [a], Takeshi Nara [a,*], Yukichi Hara [b], Takashi Aoki [a]

[a] *Department of Molecular and Cellular Parasitology, Juntendo University School of Medicine, Hongo 2-1-1, Bunkyo-ku, Tokyo 113-8421, Japan*
[b] *Department of Biochemistry and Biophysics, Tokyo Medical and Dental University, Yushima 1-5-45, Bunkyo-ku, Tokyo 113-8510, Japan*

Received 26 December 2005; received in revised form 12 April 2006; accepted 25 April 2006
Available online 16 May 2006

Abstract

Maintaining low intracellular sodium concentrations is vital for almost all organisms. Na^+ efflux is generally governed by P-type ATPases, Na^+/K^+-ATPase in animals and Na^+-ATPase, called ENA, in fungi and plants. *Trypanosoma cruzi*, which parasitizes mammalian cells, must undergo drastic adaptations to high Na^+ concentrations outside and low Na^+ concentrations inside host cells. However, *T. cruzi* Na^+ efflux pumps have not been identified. We report here the cloning and characterization of the gene encoding Na^+-ATPase in *T cruzi*, which resembled fungal and plant *ENA*s, termed *TcENA*. TcENA was a plasma membrane protein expressed throughout the parasite life cycle. The transcription level of *TcENA* was higher in insect stage epimastigotes and blood stream trypomastigotes than in intracellular amastigotes, probably reflecting the high Na^+ concentration outside the host cells. Biochemical analysis of TcENA expressed heterologously in mammalian cells demonstrated, for the fist time, that the ATPase activity of TcENA is stimulated by both Na^+ and K^+ and is insensitive to ouabain, a specific inhibitor of Na^+/K^+-ATPases. Furthermore, epimastigotes overproducing TcENA showed increased tolerance to high Na^+ stress. Our findings suggest that TcENA acts as a sodium pump and provide insights into the regulation of ion homeostasis in the parasitic protist.

Keywords: *Trypanosoma cruzi*; P-type ATPase; ENA; Ouabain; Heterologous expression; Sodium tolerance

1. Introduction

Trypanosoma cruzi is the etiological agent of Chagas' disease, which affects about 17 million people in Latin America [1]. Moreover, about 25% of the population has been estimated to be at risk [1]. *T. cruzi* has three main developmental stages: the epimastigote, which multiplies in the intestinal cavity of triatomine insects; the amastigote, which propagates by binary fission in the cytosol of mammalian cells; and the trypomastigote, the infective stage of the parasite that circulates in the blood stream of mammalian hosts [2].

Remarkably, the amastigote and trypomastigote must survive in extremely different ionic environments. That is, the trypomastigote lives in an environment containing high Na^+ (135–146 mM) and low K^+ (3.5–5.5 mM) concentrations, whereas the amastigote lives in an environment containing low Na^+ (5–15 mM) and high K^+ (140–155 mM) concentrations [3]. Thus, regulation of Na^+ and K^+ concentrations is important for parasite adaptation to the host environments and for parasite survival.

P-type ATPases are membrane proteins that can transport specific ions, including Na^+, K^+, Ca^{2+}, and H^+, across membranes against concentration gradients. Formation of a phosphorylated intermediate is characteristic of this type of enzyme during its reaction cycle [4]. P-type ATPases are responsible for maintaining various ion milieus, including the maintenance of low (<30 mM) intracellular sodium concentrations. This property is essential for all living organisms, because high internal sodium is generally toxic [5]. In mammalian cells, an ouabain-sensitive Na^+/K^+-ATPase, which exports three Na^+ ions coupled with the import of two K^+ ions per cycle, establishes an electrochemical gradient for Na^+, which drives

* Corresponding author. Tel.: +81 3 5802 1042; fax: +81 3 5800 0476.
E-mail address: tnara@med.juntendo.ac.jp (T. Nara).

0005-2736/$ - see front matter © 2006 Elsevier B.V. All rights reserved.
doi:10.1016/j.bbamem.2006.04.025

the cotransport of various solutes, including glucose, Pi, and amino acids, by symporters [6].

In plants and fungi, Na^+ efflux is essentially driven by a different type of Na^+-ATPases, called ENA [7,8]. *Saccharomyces cerevisiae* ENA has been shown to mediate tolerance to high Na^+ concentrations, and disruption of the *ENA* gene resulted in loss of viability under this condition [9]. Recently, the moss, *Physcomitrella patens*, was reported to possess two isoforms of an ENA-type ATPase (PpENA), and complementation of the *ENA*-disrupted yeast mutants with PpENA was found to rescue the defective phenotype of the former [10].

On the other hand, in parasitic protists, including *T. cruzi*, the molecular mechanism for the maintenance of intracellular Na^+ and K^+ concentrations remains unclear. In *T. cruzi*, the presence of ouabain-insensitive, Na^+-stimulated ATPase activity has been suggested but not been molecularly identified [11]. Here, we report the cloning of a gene encoding a P-type ATPase from *T. cruzi*, which is similar to ENA and termed TcENA. Biochemical analyses using a mammalian cell expression system revealed that TcENA is an ouabain-insensitive ATPase and that its activity is stimulated by both Na^+ and K^+. In addition, *T. cruzi* epimastigotes overexpressing TcENA showed significant tolerance to high Na^+ concentrations in the culture medium. Our findings provide insights into the mechanism by which the various developmental stages of *T. cruzi* maintain homeostasis to monovalent cations.

2. Materials and methods

2.1. Parasite materials

HT1080 cells, a human fibrosarcoma cell line, were infected by the mammalian stages of *T. cruzi* Tulahuen strain as described [12]. HT1080 cells, with or without *T. cruzi*, were inoculated at an initial density of $3–5 \times 10^5$/ml into DMEM (Sigma-Aldrich Japan, K.K., Japan) supplemented with 10% fetal bovine serum (FBS) in 25-cm^2 culture flasks and subcultured every 3–4 days. Trypomastigotes were collected from the subculture of infected HT1080 cells by centrifugation at 800×*g* for 5 min at 4 °C in 15-ml polypropylene tubes to remove host cells and cell debris. The resulting supernatant was centrifuged at 1500×*g* for 10 min at 4 °C, and the pellet containing trypomastigotes was washed three times with 10 ml DMEM by repeated suspension and centrifugation. The purified trypomastigotes were counted on an improved Neubauer hemocytometer and each preparation was verified to contain less than 10% amastigotes. Epimastigotes were routinely subcultured weekly in LIT medium (No. 1029, ATCC medium formulations) supplemented with 10% FBS and 10 μg/ml of hemin (Sigma-Aldrich Japan) by seeding epimastigotes at an initial density of 5×10^5/ml in tightly capped 25-cm^2 culture flasks at 26 °C.

2.2. Cloning of T. cruzi P-type ATPase gene

To obtain a gene encoding *T. cruzi* P-type ATPase, we designed degenerate primers (forward; 5′-ATGAARGGNGCNCCNGA-3′, reverse; 5′-GGRTGRTC-NCCNGTNACCAT-3′) to amplify the conserved regions of P-type ATPases, which target for the 507–621 amino acids of the human Na^+/K^+ ATPase. PCR was performed using these primers, oligo-dT-primed cDNA from trypomastigotes, and ExTaq DNA polymerase (Takara Bio Inc., Otsu, Shiga, Japan). The amplification protocol consisted of 30 cycles of denaturation at 94 °C for 30 s, annealing at 50 °C for 30 s, and extension at 72 °C for 1 min. The 370-bp PCR product was subcloned into a pCR II-TOPO vector (Invitrogen, Carlsbad, CA, USA) and sequenced, and shown to encode a portion of P-type ATPase, similar to *Saccharomyces cerevisiae ENA1*. The PCR product was labeled with digoxigenin (DIG) using DIG-PCR labeling kit (Roche Diagnostics K.K., Minato-ku, Tokyo, Japan) and the primers (forward; 5′-CGTGTAATTGAT-CTTTGCAC-3′, reverse; 5′- ACCACAATACCGGCATGTTG-3′). The DIG-labeled DNA probe was used to screen a *T. cruzi* genomic library [13], and a single positive clone containing the 18-kb insert DNA was obtained and shown to contain an open reading frame for the *T. cruzi* P-type ATPase gene. A hydropathy plot of the predicted amino acid sequence of TcENA was obtained using the TMpred program (http://www.ch.embnet.org/software/TMPRED_form.html).

2.3. Preparation of polyclonal antisera specific to TcENA

Using the primers, 5′-CGGGATCCATGTTGGAACTGCCGCCAG-3′ (sense) and 5′-CGGGATCCTCACGCCAAAACGCTCCAC-3′ (antisense), and KOD-Plus-DNA polymerase (High-Fidelity type, Toyobo Co., Ltd., Osaka, Japan), the central cytoplasmic region of *TcENA* was amplified by PCR. The PCR product was digested with *Bam*HI, subcloned into the corresponding site of the expression vector pET28a (Takara Bio), and confirmed to be free of PCR-generated errors by sequencing. The recombinant plasmid was used to transform BL21-AI™ competent *E. coli* (Invitrogen), and expression of recombinant TcENA was carried out under the conditions recommended by the manufacturer. Expression was induced by incubating the cells in 1 mM isopropyl-β-D-thiogalactopyranoside. The bacterial cells were lysed by sonication and precipitated by centrifugation at 10,000×*g* for 10 min at 4 °C. The resulting precipitate was solubilized in 8 M urea, incubated with TALON Metal Affinity Resin (BD Biosciences, San Jose, CA, USA), washed and eluted, as recommended. The resulting eluates were dialyzed extensively against phosphate-buffered saline (PBS), pH 7.2, re-precipitated, washed again with PBS, solubilized in 8 M urea/PBS, and stored at −80 °C. The purity of the recombinant TcENA was confirmed by SDS-polyacrylamide gel electrophoresis (SDS-PAGE) to be over 95%. For production of antibody specific to TcENA, BALB/c mice were each immunized with 50 μg recombinant TcENA in Freund's complete adjuvant and boosted once with 50 μg recombinant TcENA in Freund's incomplete adjuvant. Two weeks later, the immune sera were collected and used for Western blotting and indirect immunofluorescence analysis at appropriate dilutions.

2.4. Indirect immunofluorescence

T. cruzi infected HT1080 cells were grown on a cover slip in a well of a 12-well plate as described [14]. The parasite and host cells were fixed for 30 min in PBS containing 4% paraformaldehyde and permeabilized in 0.1% Triton-X 100/0.1% sodium citrate for 5 min at 4 °C. Blocking was performed in blocking solution (PBS containing 0.05% Tween 20 and 1% BSA) for 20 min, and the cells were incubated with TcENA-specific antisera in blocking solution for 18 h at room temperature. After washing with PBS, the cells were reacted with the anti-mouse FITC-conjugate, and TcENA localization was assessed under a fluorescent microscope.

2.5. Western blotting

Epimastigotes were washed with PBS and homogenized in the presence of protease inhibitor cocktail (Complete Mini, Roche Diagnostics) using cell disruption bomb (Parr Instrument Company, Moline, IL, USA) at 1,200 psi. After removal of the nuclei and cell debris by centrifugation at 1600×*g* for 10 min, the lysate was centrifuged at 150,000×*g* for 1 h. The resulting pellet and supernatant were defined as the membrane and cytosolic fractions, respectively. The proteins were separated by SDS-PAGE and blotted to PVDF membranes, which were incubated with TcENA-specific antibody. Bound primary antibodies were visualized with alkaline phosphatase-conjugated secondary antibody and CSPD (Roche Diagnostics).

2.6. Northern blotting

Total RNA was extracted from epimastigotes, trypomastigotes, or amastigotes using Trizol® reagent (Invitrogen) according to the manufacturer's recommendations, and Northern hybridization was performed as

described [12]. Briefly, the RNA samples were electrophoresed on 1% agarose gels, blotted to nylon membranes (Roche Diagnostics), and hybridized with the TcENA-specific DNA probe, which was DIG-labeled using PCR probe Synthesis Kit (Roche Diagnostics) in the presence of the primers, 5′-CACCATGTCGGATTCGAAAGAGC-3′ and 5′-TTAGCGGTA-CACCATATTCTTGC-3′, and the TcENA-carrying plasmid DNA as a template. Chemiluminescent detection of the hybridization signals was performed using CSPD (Roche Diagnostics).

2.7. Expression of TcENA

The full-length TcENA cDNA was PCR amplified using the primers, 5′-CTCGAGATGTCGGATTCGAAAGAGCT-3′ (sense) and 5′-TTTACC-GGTCCACGCCTCTTCTTTTTCCTCT-3′ (antisense), KOD-Plus-DNA polymerase, and cDNA synthesized from epimastigote total RNA. The PCR product was cloned into pCRII-TOPO and restricted with *Xho*I and *Age*I. The resulting cDNA fragment was cloned into the *Xho*I and *Age*I sites of the mammalian expression vector pEGFP-N1 (Clontech, Takara Bio Inc., Otsu, Shiga, Japan), which allows carboxyl terminal fusion with EGFP (pEGFP-TcENA). FreeStyle™ 293-F cells (Invitrogen) were cultured in 125-ml polycarbonate Erlenmeyer flasks containing 30 ml of FreeStyle™ 293 Expression medium to a density of 5×10^5 cells/ml. The cells were transfected with 30 μg pEGFP-TcENA using 40 μl of LipofectAMINE™ 2000 (Invitrogen) according to the manufacturer's instructions. The cells were incubated for 48 h and transferred to fresh medium supplemented with 1 mg/ml G418 sulfate (cell culture tested, Calbiochem, EMD Biosciences, Inc., La Jolla, CA, USA) to select transformed cells, changing the medium every 3 days. Four weeks after the start of continuous cultures, the transformed cells expressing EGFP were established and used for further experiments.

2.8. Measurement of ATPase activity

The FreeStyle™ 293-F cells expressing the TcENA-EGFP fusion protein were harvested by centrifugation at 100×*g* for 5 min, and suspended in 10 volumes of ice-cold homogenization buffer (250 mM sucrose, 50 mM imidazole–HCl (pH 7.0), 5 mM sodium azide, and 2 mM EDTA), and homogenized in a Teflon-coated Dounce homogenizer with 10 gentle strokes. The homogenate was centrifuged at 5000×*g* for 10 min to remove nuclei, mitochondria, and cell debris. The supernatant was centrifuged at 47,000×*g* for 30 min and the resulting supernatants and precipitates were designated the cytosolic and membrane fractions, respectively. The pellet was suspended in homogenization buffer containing 0.065% sodium deoxycholate (Sigma, St. Louis, MO, USA). ATPase activity was measured as described [15]. The reaction was initiated by adding 30 μg proteins to 1 ml assay mixture containing 50 mM Tris–HCl pH 7.6, 4 mM $MgCl_2$, 2 mM EGTA, 3 mM Tris–ATP, 1 mM phosphoenolpyruvate, 10 U/ml pyruvate kinase (Wako Pure Chemical Industries Co., Tokyo, Japan), 30 U/ml lactate dehydrogenase (Wako Pure Chemical Industries), 0.2 mM NADH, 10 nM bafilomycin (an inhibitor of V-type ATPase, Sigma), 100 nM tapsigargin (an inhibitor of sarcoplasmic reticulum Ca^{2+}-ATPase, Sigma), 5 mM sodium azide, 130 mM NaCl, and 20 mM KCl. Sodium orthovanadate (Calbiochem) and ouabain (Sigma) were used as inhibitors of P-type ATPase and Na^+/K^+-ATPase, respectively. Choline chloride (Sigma) was used to keep the ion strength in the assay mixture. The rate of reaction was determined as the steady-state value of dA_{340}/dt at 37 °C for 10 min. ATPase activity was calculated based on the extinction coefficient of NADH ($\varepsilon=6.22\ mM^{-1}\ cm^{-1}$).

2.9. Expression of EGFP-tagged TcENA in T. cruzi

The vector backbone of pEGFP-TcENA was replaced by that of the trypanosomatid shuttle vector, pTREX [16]. Briefly, The DNA fragment carrying the *TcENA-EGFP* fused gene was amplified from pEGFP-TcENA by PCR using the primers, 5′-AAACTAGTATGTCGGATTCGAAAGAGCT-3′ (sense) and 5′-TTCTCGAGTTAAGCGTAATCTGGAACATCGTATGGG-TACTTGTACAGCTCG-3′ (antisense), and KOD-Plus- DNA polymerase. The PCR product was subcloned into pCR II-TOPO, digested with *Xho*I, and cloned into the *Xho*I site of pTREX. The resulting recombinant plasmid, designated pTREX/TcENA-EGFP, was used for transformation of *T. cruzi* epimastigotes by electroporation using a Gene Pulser apparatus (Bio-Rad Laboratories, Hercules, CA, USA) with three pulses at 400 V and 500 μF [17]. The stable transformants were selected by incubating the cells for 60 days in LIT medium containing 500 μg/ml G418. Expression of TcENA-EGFP in the transformed epimastigotes was detected by fluorescent microscopy.

3. Results

3.1. Isolation and nucleotide sequence analysis of the TcENA gene

We designed degenerate primers based on the conserved amino acid sequences of animal Na^+/K^+-ATPases and fungal *ENA*-type ATPases. Using PCR, we obtained a product of approximately 370 bp, with a deduced amino acid sequence similar to those of fungal ENA and the calcium motive P-type ATPases of trypanosomatids (data not shown). This DNA fragment was DIG-labeled and used to screen a *T. cruzi* genomic library, resulting in the isolation of a clone containing an 18-kb insert encoding full-length *T. cruzi* P-type ATPase DNA, which we designated *TcENA*.

The open reading frame of *TcENA* consisted of 3,117 nucleotides, encoding 1,039 amino acids with a calculated molecular mass of 120 kDa (GenBank™ AB107891, Fig. 1). TcENA contains the sequence DKTGTLT, a motif of the phosphorylation site conserved in all P-type ATPases. The hydropathy plot of TcENA shows 10 hydrophobic regions of sufficient length to span the membrane, indicating the presence of ten transmembrane segments (Fig. 2).

The deduced amino acid sequence of TcENA shared identity with the sequences of the putative calcium motive P-type ATPases of *Leishmania donovani* (66% identity, GenBank™ AF067495) and *T. brucei* (71%, Tb09.244.2570 in; http://www.sanger.ac.uk/Projects/T_brucei/) and was identical to that of putative calcium motive P-type ATPase (Tc00.1047053510769.120 in; http://tcruzidb.org/). We identified an additional ortholog of TcENA (Tc00.1047053506241.70 in; http://tcruzidb.org/) in the *T. cruzi* genome database, which had a 99.3% amino acid sequence identity to that of TcENA.

The TcENA sequence was similar to those of various sodium-pumping ATPases, ENAs, including PpENA1 of the moss *Physcomitrella patens* (38% identity, GenBank™ AJ564254, see Fig. 1), cta3 of *Schizosaccharomyces pombe* (35%, GenBank™ J05634), and ENA1 of *Saccharomyces cerevisiae* (34%, GenBank™ U24069). Based on sequence homology, P-type ATPases can be divided into five groups [8]. Although the trypanosomatid ATPases were annotated as putative "calcium motive P-type ATPases" without biochemical analysis and their amino acid sequences are less identical to that of fungal and plant ATPases, the phylogenetic analyses suggested that the trypanosomatid, plant, and fungal ATPases are phylogenetically related and belong to type IID ATPases [10,18]. Thus, TcENA appears to be a type IID ATPase and is likely to play a role in sodium transport.

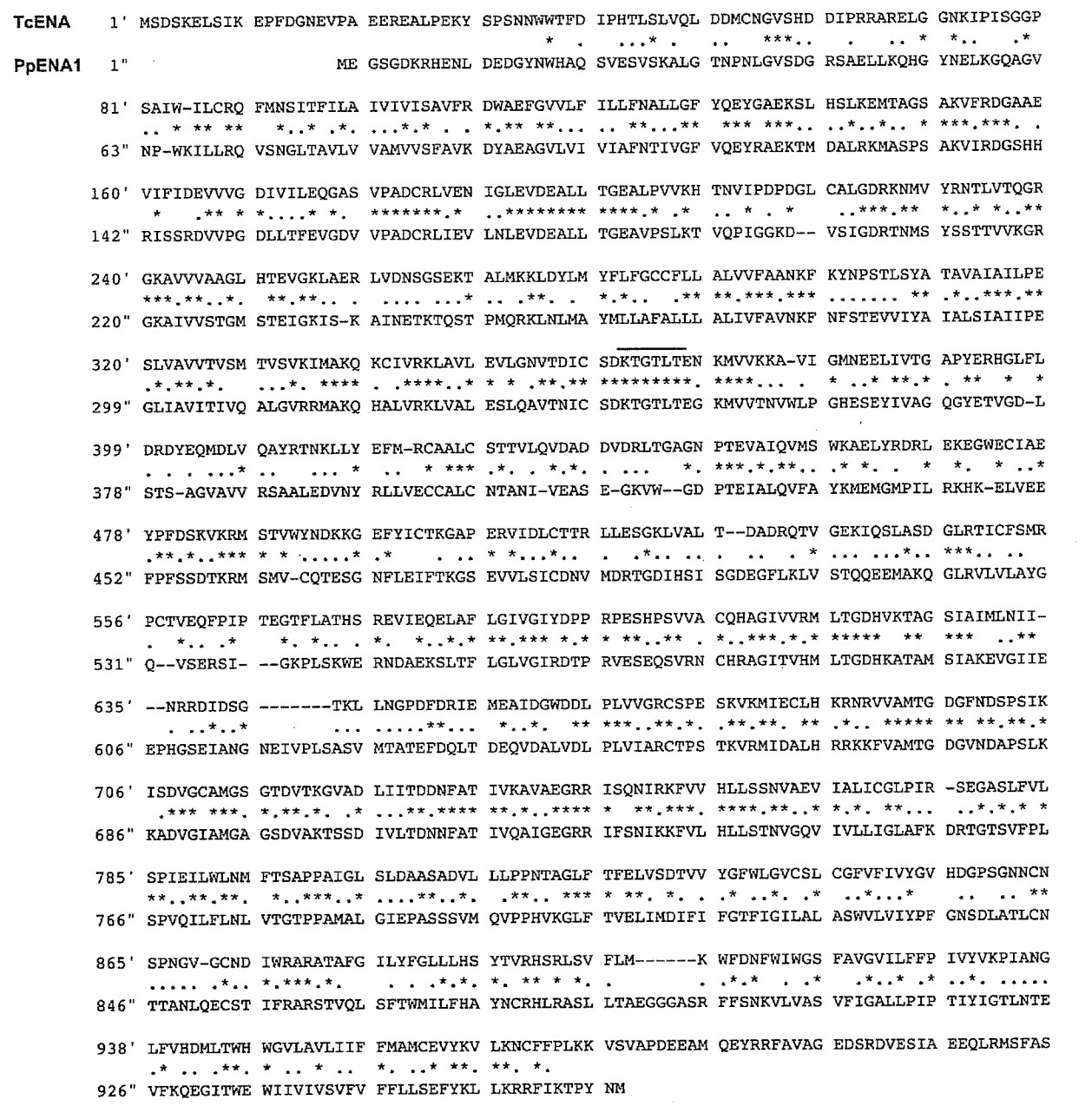

Fig. 1. Alignment of the deduced amino acid sequences of the ENA-type ATPases of *Trypanosoma cruzi* (TcENA, GenBank™ AB107891) and *Physcomitrella patent* (PpENA1, GenBank™ AJ564254). Asterisks and dots represent identical and equivalent amino acids, respectively. The phosphorylation site, characteristic of P-type ATPases, is underlined.

3.2. Transcription of TcENA gene at different stages of T. cruzi

To analyze transcription level of the *TcENA* gene, we performed Northern hybridization on total RNAs from the three *T. cruzi* stages, trypomastigotes, epimastigotes, and amastigotes, using the TcENA-specific DNA probe (Fig. 3). Since it is difficult to separate amastigotes from host cells, we used total RNA from heavily parasitized host cells as amastigote RNA (lane A, Fig. 3A).

The TcENA transcript was present as a band of approximately 4.5 kb in all three *T. cruzi* stages, with additional faint bands at higher molecular weight in epimastigote. There were no bands in host RNA (Fig. 3B). The transcription level of TcENA differed by developmental stage. When the amount of RNA was normalized relative to the signal intensity of *T. cruzi* 5S rRNA, the transcription level of TcENA was 1.8-fold higher in trypomastigotes than in amastigotes (Fig. 3B).

3.3. Localization of TcENA in the plasma membrane of T. cruzi

We investigated expression of TcENA in epimastigote by Western blotting. Since fungal ENA is localized on the plasma

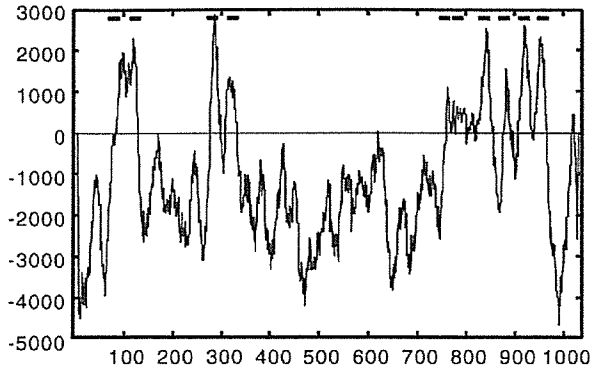

Fig. 2. Hydropathy plot of TcENA based on the TMpred program (http://www.ch.embnet.org/software/TMPRED_form.html). Possible transmembrane regions are indicated by the horizontal bars at the top of the frame.

membrane, we prepared cytosolic and membrane fractions of *T. cruzi* epimastigotes and reacted each with antisera raised against recombinant TcENA (Fig. 4A). We observed the expected 120 kDa band only in the membrane fraction, suggesting that, like other P-type ATPases, TcENA is expressed as a membrane protein.

We also assayed the subcellular localization of TcENA by indirect immunofluorescence in trypomastigotes (Fig. 4B) and amastigotes (Fig. 4C). In both developmental stages, the anti-TcENA antibody reacted predominantly with the parasite plasma membrane. In *S. cerevisiae*, ENA1 is required for the efflux of sodium ions and is localized in the plasma membrane [19]. These results suggest that TcENA is localized in the plasma membrane of *T. cruzi* and is most likely to function as an efflux pump of monovalent cations, thus maintaining ion homeostasis in the parasite.

3.4. Heterologous expression of TcENA in eukaryotic cells

As *S. cerevisiae* B31 strain (*ena1*Δ::*HIS3*::*ena4 nha1*Δ::*LEU2*) does not carry the two major Na^+ efflux systems, ENA

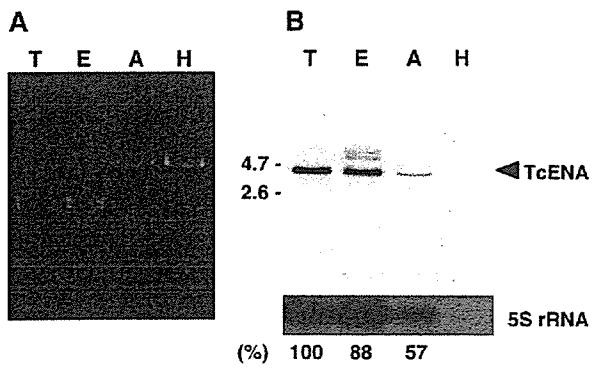

Fig. 3. Expression of *TcENA* mRNA. (A) Ten μg total RNA isolated from trypomastigotes (T), epimastigotes (E), amastigotes-infected cells (A), and host cells (H) were electrophoresed on agarose gels and stained with ethidium bromide. (B) RNAs of panel A were blotted to nylon membranes and hybridized with DIG-labeled DNA probes specific for the *TcENA* (upper panel) and *5S rRNA* (lower panel) genes. The molecular size in kilobases is indicated on the left. At the bottom, shown are the transcription levels of *TcENA*, normalized to *5S rRNA*.

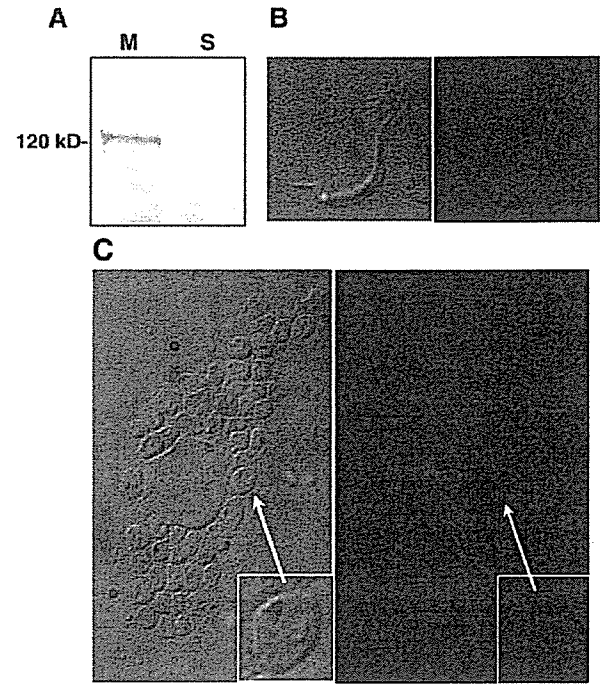

Fig. 4. Localization of TcENA in *T. cruzi*. (A) Membrane (M) and soluble (S) fractions were prepared from epimastigotes, resolved on SDS-PAGE, and reacted with anti-TcENA antibody. Six μg of the proteins were loaded onto each lane. kDa; kilodaltons. (B, C) Detection of TcENA in trypomastigotes (B) and intracellular amastigotes (C). The parasites were fixed, incubated with TcENA-specific antisera, and stained with FITC-labeled secondary antibodies (right panels). The left panels represent differential interference contrast (DIC) images. The inset in (C) indicates a single amastigote (an arrow).

and Na^+/H^+ antiporter, it is more sensitive to salt stress [20]. Expression of *P. patens* ENA in the B31 strain allowed survival of the transformants under conditions of high Na^+ [10]. Thus, we assayed whether expression of TcENA could complement the B31 phenotype. When we tried to express TcENA using pDR195, a plasmid that carries the *PMA1* promoter [21], as well as in various commercially available vectors, none of these transformants showed tolerance to high Na^+ (data not shown). In addition, when we attempted to transform *S. cerevisiae* G19 strain (*ena1*Δ::*HIS3*::*ena4*) [22] with *TcENA* gene, we failed to detect the phenotype (data not shown).

We therefore attempted to express TcENA using a mammalian expression system, in which FreeStyle™ 293-F cells, a derivative of the human 293 cell line, were transformed using the recombinant plasmid carrying the *TcENA-EGFP* fusion gene (Fig. 5). FreeStyle™ 293-F cells were transfected with the plasmid by lipofection and continuously cultured for 4 weeks in the presence of 1 mg/ml G418 to obtain stable transformants. In human cells, fluorescence of TcENA-EGFP was detected in the plasma membrane, indicating that TcENA-EGFP was successfully expressed as a plasma membrane protein (Fig. 5A). We therefore used this heterologous expression system to determine the enzymatic properties of TcENA.

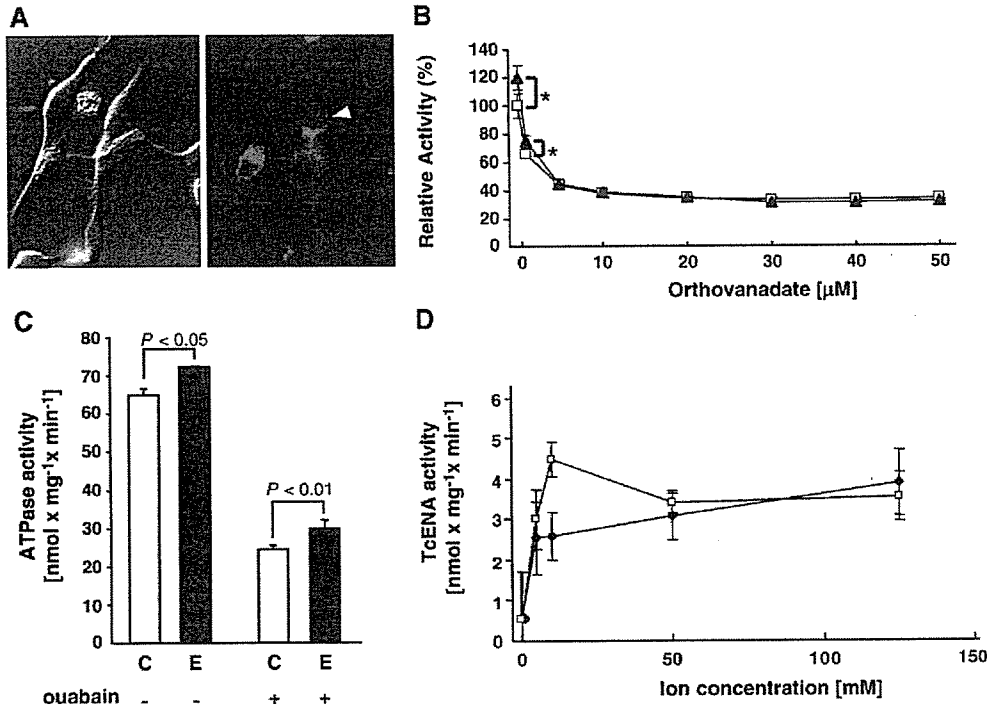

Fig. 5. Expression of TcENA in a human cell line. (A) Direct fluorescence localization of EGFP-tagged TcENA in the plasma membrane of FreeStyle™ 293-F cells. The arrowhead indicates a monolayer cell demonstrating fluorescence on its surface. Left, DIC image; right, fluorescence image. (B) Measurement of ATPase activity in the plasma membrane fraction of TcENA-expressing (triangle) and control (square) cells in the presence of sodium orthovanadate. Values are mean±S.D. of three independent experiments. An asterisk represents the statistical significance of $P<0.05$. (C) Measurement of ATPase activity in the plasma membrane fraction of TcENA-expressing (E) and control (C) cells in the absence or presence of 1 mM ouabain. (D) Effect of different concentrations of Na^+ (diamond) and K^+ (square) on TcENA activity in the presence of 1 mM ouabain. The TcENA-specific ATPase activity was shown by subtracting the activity of the control cells from that of the TcENA-expressing cells. The ionic strength was kept constant by adding choline chloride and the concentrations of choline plus either Na^+ or K^+ were adjusted to be 140 mM. Values are mean±S.D. of three independent experiments.

3.5. Monovalent cation-stimulated ATPase activity of TcENA

We sought first to measure the ATPase activity in the membrane fractions of transformed FreeStyle™ 293-F cells expressing TcENA-EGFP or EGFP (control) in the presence of 130 mM Na^+ and 20 mM K^+. To measure the monovalent cation-specific ATPase activity, calcium ATPases were inhibited by EGTA, and the contaminating activities of V-type ATPases and sarcoplasmic reticulum Ca^{2+}-ATPase were eliminated by the addition of bafilomycin and thapsigargin, respectively.

In the absence of orthovanadate, a specific inhibitor of P-type ATPases, we found the significantly higher ATPase activity in the membrane fraction of the TcENA-producing cells than that of the control ($P<0.05$, indicated by an asterisk in Fig. 5B), whereas overall ATPase activity of both membrane fractions was high. In the presence of orthovanadate, ATPase activity of both cells declined in a dose-dependent manner, and nearly 30% of the ATPase activity remained even in the presence of 50 μM orthovanadate, probably due to the contaminating non P-type ATPases in our membrane fractions (Fig. 5B). When the concentration of orthovanadate was ≥5 μM, there was no significant difference of ATPase activity between the experimental and control cells. These results indicate that TcENA possessed orthovanadate-sensitive ATPase activity, which is characteristic to a P-type ATPase, and that the ATPase activity of TcENA was stimulated by either Na^+ or K^+, or both cations.

We confirmed the presence of Na^+/K^+-ATPase activity, a plasma membrane marker, in our membrane fractions, in that addition of ouabain, a specific Na^+/K^+-ATPase inhibitor, drastically reduced the ATPase activity of TcENA-expressing and control cells (Fig. 5C). The residual ATPase activity (approximately 25 nmol/mg/min) of the control cells in the presence of ouabain (1 mM) was comparable to that in the presence of orthovanadate (≥30 μM), suggesting that the orthovanadate-sensitive ATPase activity of the control cells can be attributed to the native Na^+/K^+-ATPase. It is important to note that TcENA-expressing cells showed significantly higher ATPase activity than did control cells, both in the presence and in absence of ouabain ($P<0.01$, Fig. 5C). These results indicate that TcENA is an ouabain-insensitive, monovalent cation-specific ATPase.

Next, we addressed identification of the cation associated with TcENA ATPase activity, using a basal assay mixture containing 1 mM ouabain and 15 mM NH_4^+ instead of K^+ [23]. In this assay, the ionic strength was kept constant by adding choline chloride. The ATPase activity of the TcENA-expressing cells was significantly stimulated by either Na^+ or K^+ alone in a dose-dependent manner (Fig. 5D). Theses results clearly indicate that TcENA is stimulated not only by Na^+ but also

by K^+. At the lower concentrations of the monovalent cations (10 mM), we observed higher ATPase activity for K^+ than for Na^+, while the reason was not clear.

3.6. Tolerance to high Na^+ stress in TcENA-overexpressing *T. cruzi*

Using genetically modified epimastigotes, we sought to determine the physiological role of TcENA in *T. cruzi*. Epimastigotes were transfected with a trypanosomal expression plasmid, pTREX, carrying the *TcENA-EGFP* fusion gene. Expression of the TcENA-EGFP protein in the resulting transformants (TcENA-*T. cruzi*) was confirmed by Western blot and indirect fluorescence analyses using the anti-TcENA antibody (data not shown). In LIT medium, TcENA-*T. cruzi* displayed a slightly faster growth rate than the control cells, which had been transformed with pTREX alone (Fig. 6A).

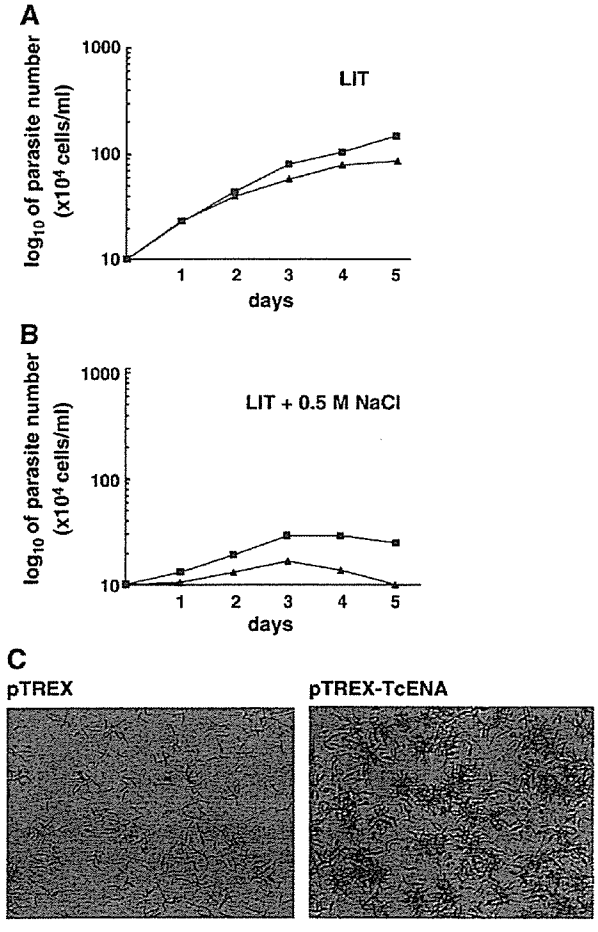

Fig. 6. Phenotypic analyses of TcENA-overexpressing *T. cruzi* epimastigotes under conditions of high Na^+ stress. Growth curve of TcENA-overexpressing (closed squares) and control (closed triangles) epimastigotes in the absence (A) or presence (B) of 0.5 M NaCl. Each data point represents the mean of quadruplicate determinations. (C) Microscopic observation of the TcENA-overexpressing (right) and control (left) epimastigotes. Note that epimastigotes of both groups attached to the bottom of the culture flask, but that the rosette-formation was only observed in TcENA-overexpressers. The video images are also available on line (Supplementary video).

We proceeded to test the susceptibility of TcENA-*T. cruzi* to high Na^+ stress. Both the TcENA-*T. cruzi* and control epimastigotes were cultured in LIT medium containing 500 mM NaCl, and parasite growth was monitored for 5 days. The parasite growth was gradually suppressed in both the experimental and control epimastigotes, most likely due to high Na^+ concentration in the medium (Fig. 6B). Interestingly, the number of TcENA-*T. cruzi* epimastigotes was significantly higher than that of control epimastigotes, indicating that overexpression of TcENA leads to tolerance to high Na^+ stress.

We found that the motility and behavioral patterns differed for TcENA-*T. cruzi* and control epimastigotes (Supplementary video is available on line). After 14 days in cultivation, control epimastigotes became less motile and attached individually to the bottom of the culture flask (Fig. 6C). In contrast, TcENA-epimastigotes showed intense movement and formed rosette-like aggregations, similar to those observed in normal cultivation. These findings indicate that overexpression of TcENA in *T. cruzi* confers salt tolerance on the parasite, which is most likely driven by accelerated Na^+ efflux.

4. Discussion

For many parasitic organisms, the crucial steps in their life cycle include the transmission between hosts and entry into their definitive habitats. These changed are accompanied by rapid and drastic changes in the environmental conditions of the parasite. Intracellular parasites, such as *T. cruzi*, especially require adaptation to different ionic environments. *T. cruzi* has a complex life cycle, which includes the obligatory mammalian stages in the host cell cytosol and in the blood stream. In these two environments, the parasite lives under conditions of extremely different Na^+ and K^+ balance.

In the present study, we identified a gene encoding Na^+-ATPase in *T. cruzi*, which we termed *TcENA*. The deduced amino acid sequence of TcENA showed significant similarity with those of fungal and plant ENA, which have been characterized as Na^+ and K^+ efflux pumps. A search of the *T. cruzi* genome sequence database revealed the presence of two *TcENA* genes, which share a 99.3% amino acid sequence identity. *T. cruzi* strain CL Brener, the reference strain in the *T. cruzi* genome project, has a hybrid genome comprised of two distantly related *T. cruzi* lineages [24]. The presence of two *TcENA* genes with sequence variations may reflect the hybrid nature of the CL Brener genome.

Previous analyses of fungal and plant ENAs have been limited to a survey of defective phenotypes in *ENA*-disrupted yeast mutants and to phenotypic complementation using heterologous expression [25,26]. Therefore, biochemical properties of ENAs, including their ATPase activities and the ionic stimulants, had not yet been determined. In the present study, we established a unique assay system for TcENA using a mammalian expression system and an established enzyme assay [15], since the plasma membrane fraction of *T. cruzi* contains high levels of H^+-ATPase activity, which would mask its Na^+-ATPase activity [27]. This system provides several advantages for analyses of ENA-type ATPases, since mammals lack ENA;

mammalian P-type ATPases have been well characterized; and inhibitors of various type of ATPases are available.

Using this assay system, we could demonstrate for the first time that TcENA possessed the orthovanadate-sensitive ATPase activity, which is characteristic to P-type ATPases. In the presence of ouabain, ATPase activity of the membrane fraction of TcENA-producing cell was significantly higher than that of the control cells, indicating that TcENA is an ouabain-insensitive ATPase. Furthermore, the TcENA-specific ATPase activity was stimulated in the presence of either Na^+ or K^+, dependent on the concentration of cations. Dependence of the ATPase activity of TcENA on the ion strength is unlikely as the ionic strength was kept constant. Since Na^+/K^+-ATPase does not function in the absence of either Na^+ or K^+, these results provide evidence that TcENA is actually expressed in the transformed cells and possesses the Na^+- or K^+-stimulated ATPase activity. On the other hand, our membrane fractions showed the high level of the background ATPase activities, probably due to the contaminating non P-type ATPases, such as membrane-associated, cytoskeletal actin. Further improvement of the assay system, especially for reducing the background ATPase activities, is necessary to determine the exact enzyme properties of TcENA.

Our biochemical analysis clearly showed that TcENA is an ouabain-insensitive and Na^+- or K^+-stimulated ATPase. The presence of ouabain-insensitive, Na^+-stimulated ATPase activity has been previously suggested in *T. cruzi*, but not been molecularly identified [11,27]. Thus, the latter activity can most likely be attributed to TcENA. An orthologous gene of *TcENA* is conserved in other trypanosomatids, including *L. donovani* and *T. brucei* [18], which are the pathogens for the important tropical diseases, Kala-azar and African sleeping sickness, respectively. The presence of an ENA-type ATPase in trypanosomatids and its absence from humans may provide insights into the trypanosomatid ENA-type ATPases as drug targets in the treatment of trypanosome infections.

Although *TcENA* is expressed throughout the *T. cruzi* life cycle, its transcription level was higher in epimastigotes and trypomastigotes than in amastigotes. These findings are in agreement with the facts that epimastigotes and trypomastigotes can live in conditions of high Na^+ concentrations. Trypomastigotes live in the blood stream, which contains 145 mM Na^+, and epimastigotes grow well in medium containing the same Na^+ concentration. In addition, we found that epimastigotes overexpressing TcENA are active in medium containing extremely high concentration of Na^+, strongly suggesting that TcENA functions as a sodium efflux pump and confers tolerance to high Na^+. Amastigotes, however, live in the host cell cytosol, where the concentration of Na^+ is much lower, suggesting that, in this stage, TcENA has less importance in Na^+ efflux. Thus, differences in transcription level between the extracellular and intracellular forms may reflect differences in environmental Na^+ concentration.

Similar to other ENAs, we found that TcENA is stimulated not only by Na^+ but also by K^+. Although the physiological importance of the ability of *T. cruzi* TcENA to extrude K^+ is unclear, it is possible to speculate that K^+ efflux is necessary for intracellular amastigotes. Amastigotes live in the host cell cytosol and are exposed to higher concentrations of K^+ than in the blood stream . It is noteworthy that amastigotes express K^+ channels, which allow import of K^+ across the plasma membrane [27]. Thus, TcENA may play dual roles in parasite development. In epimastigotes and trypomastigotes, it may function as a sodium pump, whereas in amastigotes, it may be involved in the maintenance of K^+ concentration. That is, K^+ homeostasis may be balanced by import via K^+ channels and export via TcENA.

Fungal ENAs are thought to have different preferences for Na^+ and K^+ [28]. For example, *Neurospora crassa* ENA appears to be associated with Na^+ efflux, whereas *S. pombe* ENA (cta3) seems to be a K^+-ATPase [28]. We found that TcENA displayed higher ATPase activity for K^+ than for Na^+ at the lower concentration of cations (10 mM). This may reflect a difference in transporting efficiency, while its physiological significance is unclear.

In addition to the ouabain-insensitive TcENA, the presence of an ouabain-sensitive sodium pump in *T. cruzi* has been suggested [27]. To determine whether the latter activity could be attributed to Na^+/K^+ ATPase, we extensively searched for an ortholog of mammalian Na^+/K^+ ATPase in the genome sequence databases of trypanosomatids, including *T. cruzi*, but we were unable to find any. Further analyses are necessary to understand the physiological roles of TcENA, using parasites lacking the *TcENA* gene, as well as the mechanism of regulation of Na^+ and K^+ homeostasis in *T. cruzi*.

Acknowledgements

We thank Drs. Maria Curto and Mariano Levin for providing us with the pTREX vector, Begoña Benito and Alonso Rodríguez-Navarro for *S. cerevisiae* B31 strain, Serge Potier for *S. cerevisiae* G19 strain, and Doris Rentsch for the yeast vector pDR195. This work was supported in part by Grants-in-Aid for Scientific Research (Nos. 17590377 and 17390123) from the Ministry of Education, Culture, Sports, Science, and Technology of Japan. K.I, M.H, and T.A were supported by a Grant-in-Aid for the 21st Century COE Research from the Ministry of Education, Culture, Sports, Science, and Technology of Japan.

Appendix A. Supplementary data

Supplementary data associated with this article can be found, in the online version, at doi:10.1016/j.bbamem.2006.04.025.

References

[1] J.A. Urbina, R. Docampo, Specific chemotherapy of Chagas disease: controversies and advances, Trends Parasitol. 19 (2003) 495–501.
[2] Z. Brener, Biology of *Trypanosoma cruzi*, Annu. Rev. Microbiol. 27 (1973) 347–382.
[3] J.A. King, J.C. Fray, Hydrogen and potassium regulation of (pro)renin processing and secretion, Am. J. Physiol. 267 (1994) F1–F12.
[4] W. Kühlbrandt, Biology, structure and mechanism of P-type ATPases, Nat. Rev., Mol. Cell Biol. 5 (2004) 282–295.

[5] K.M. Hahnenberger, Z. Jia, P.G. Young, Functional expression of the *Schizosaccharomyces pombe* Na^+/H^+ antiporter gene, sod2, in *Saccharomyces cerevisiae*, Proc. Natl. Acad. Sci. U. S. A. 93 (1996) 5031–5036.
[6] J.H. Kaplan, Biochemistry of Na,K-ATPase, Annu. Rev. Biochem. 71 (2002) 511–535.
[7] R. Haro, B. Garciadeblas, A. Rodriguez-Navarro, A novel P-type ATPase from yeast involved in sodium transport, FEBS Lett. 291 (1991) 189–191.
[8] K.B. Axelsen, M.G. Palmgren, Evolution of substrate specificities in the P-type ATPase superfamily, J. Mol. Evol. 46 (1998) 84–101.
[9] B. Garciadeblás, F. Rubio, F.J. Quintero, M.A. Bañuelos, R. Haro, A. Rodríguez-Navarro, Differential expression of two genes encoding isoforms of the ATPase involved in sodium efflux in *Saccharomyces cerevisiae*, Mol. Gen. Genet. 236 (1993) 363–368.
[10] B. Benito, A. Rodriguez-Navarro, Molecular cloning and characterization of a sodium-pump ATPase of the moss *Physcomitrella patens*, Plant J. 36 (2003) 382–389.
[11] C. Caruso-Neves, M. Einicker-Lamas, C. Chagas, M.M. Oliveira, A. Vieyra, A.G. Lopes, Ouabain-insensitive Na(+)-ATPase activity in *Trypanosoma cruzi* epimastigotes, Z. Naturforsch. [C] 54 (1999) 100–104.
[12] M. Hashimoto, J. Nakajima-Shimada, T. Aoki, *Trypanosoma cruzi* posttranscriptionally up-regulates and exploits cellular FLIP for inhibition of death-inducing signal, Mol. Biol. Cell 16 (2005) 3521–3528.
[13] T. Nara, Y. Hirayama-Noguchi, G. Gao, E. Murai, T. Annoura, T. Aoki, Diversity of aspartate carbamoyltransferase genes of *Trypanosoma cruzi*, Int. J. Parasitol. 33 (2003) 845–852.
[14] J. Nakajima-Shimada, C. Zou, M. Takagi, M. Umeda, T. Nara, T. Aoki, Inhibition of Fas-mediated apoptosis by *Trypanosoma cruzi* infection, Biochim. Biophys. Acta 1475 (2000) 175–183.
[15] J.G. Nørby, Coupled assay of Na^+,K^+-ATPase activity, Methods Enzymol. 156 (1988) 116–119.
[16] M.P. Vazquez, M.J. Levin, Functional analysis of the intergenic regions of TcP2beta gene loci allowed the construction of an improved *Trypanosoma cruzi* expression vector, Gene 239 (1999) 217–225.
[17] T. Annoura, T. Nara, T. Makiuchi, T. Hashimoto, T. Aoki, The origin of dihydroorotate dehydrogenase genes of kinetoplastids, with special reference to their biological significance and adaptation to anaerobic, parasitic conditions, J. Mol. Evol. 60 (2005) 113–127.
[18] J.K. Stiles, Z. Kucerova, B. Sarfo, C.A. Meade, W. Thompson, P. Shah, L. Xue, J.C. Meade, Identification of surface-membrane P-type ATPases resembling fungal K(+)- and Na(+)-ATPases, in *Trypanosoma brucei*, *Trypanosoma cruzi* and *Leishmania donovani*, Ann. Trop. Med. Parasitol. 97 (2003) 351–366.
[19] S. Siniossoglou, E.C. Hurt, H.R. Pelham, Psr1p/Psr2p, two plasma membrane phosphatases with an essential DXDX(T/V) motif required for sodium stress response in yeast, J. Biol. Chem. 275 (2000) 19352–19360.
[20] M.A. Bañuelos, H. Sychrova, C. Bleykasten-Grosshans, J.L. Souciet, S. Potier, The Nha1 antiporter of *Saccharomyces cerevisiae* mediates sodium and potassium efflux, Microbiology 144 (Pt. 10) (1998) 2749–2758.
[21] D. Rentsch, M. Laloi, I. Rouhara, E. Schmelzer, S. Delrot, W.B. Frommer, NTR1 encodes a high affinity oligopeptide transporter in Arabidopsis, FEBS Lett. 370 (1995) 264–268.
[22] M.A. Bañuelos, R.D. Klein, S.J. Alexander-Bowman, A. Rodriguez-Navarro, A potassium transporter of the yeast *Schwanniomyces occidentalis* homologous to the Kup system of *Escherichia coli* has a high concentrative capacity, EMBO J. 14 (1995) 3021–3027.
[23] J.G. Nørby, Studies on a coupled enzyme assay for rate measurements of ATPase reactions, Acta Chem. Scand. 25 (1971) 2717–2726.
[24] C.A. Machado, F.J. Ayala, Sequence variation in the dihydrofolate reductase-thymidylate synthase (DHFR-TS) and trypanothione reductase (TR) genes of *Trypanosoma cruzi*, Mol. Biochem. Parasitol. 121 (2002) 33–47.
[25] M.A. Bañuelos, F.J. Quintero, A. Rodríguez-Navarro, Functional expression of the ENA1(PMR2)-ATPase of *Saccharomyces cerevisiae* in *Schizosaccharomyces pombe*, Biochim. Biophys. Acta 1229 (1995) 233–238.
[26] B. Benito, F.J. Quintero, A. Rodriguez-Navarro, Overexpression of the sodium ATPase of *Saccharomyces cerevisiae*: conditions for phosphorylation from ATP and Pi, Biochim. Biophys. Acta 1328 (1997) 214–226.
[27] N. Van Der Heyden, R. Docampo, Proton and sodium pumps regulate the plasma membrane potential of different stages of *Trypanosoma cruzi*, Mol. Biochem. Parasitol. 120 (2002) 127–139.
[28] B. Benito, B. Garciadeblas, A. Rodriguez-Navarro, Potassium- or sodium-efflux ATPase, a key enzyme in the evolution of fungi, Microbiology 148 (2002) 933–941.

TLR-Dependent Induction of IFN-β Mediates Host Defense against *Trypanosoma cruzi*[1]

Ritsuko Koga,* Shinjiro Hamano,† Hirotaka Kuwata,* Koji Atarashi,* Masahiro Ogawa,* Hajime Hisaeda,† Masahiro Yamamoto,‡ Shizuo Akira,‡ Kunisuke Himeno,† Makoto Matsumoto,* and Kiyoshi Takeda[2]*

Host resistance to the intracellular protozoan parasite *Trypanosoma cruzi* depends on IFN-γ production by T cells and NK cells. However, the involvement of innate immunity in host resistance to *T. cruzi* remains unclear. In the present study, we investigated host defense against *T. cruzi* by focusing on innate immunity. Macrophages and dendritic cells (DCs) from MyD88$^{-/-}$TRIF$^{-/-}$ mice, in which TLR-dependent activation of innate immunity was abolished, were defective in the clearance of *T. cruzi* and showed impaired induction of IFN-β during *T. cruzi* infection. Neutralization of IFN-β in MyD88$^{-/-}$ macrophages led to enhanced *T. cruzi* growth. Cells from MyD88$^{-/-}$IFNAR1$^{-/-}$ mice also showed impaired *T. cruzi* clearance. Furthermore, both MyD88$^{-/-}$TRIF$^{-/-}$ and MyD88$^{-/-}$IFNAR1$^{-/-}$ mice were highly susceptible to in vivo *T. cruzi* infection, highlighting the involvement of innate immune responses in *T. cruzi* infection. We further analyzed the molecular mechanisms for the IFN-β-mediated antitrypanosomal innate immune responses. MyD88$^{-/-}$TRIF$^{-/-}$ and MyD88$^{-/-}$IFNAR1$^{-/-}$ macrophages and DCs exhibited defective induction of the GTPase IFN-inducible p47 (IRG47) after *T. cruzi* infection. RNA interference-mediated reduction of IRG47 expression in MyD88$^{-/-}$ macrophages resulted in increased intracellular growth of *T. cruzi*. These findings suggest that TLR-dependent expression of IFN-β is involved in resistance to *T. cruzi* infection through the induction of IRG47. *The Journal of Immunology,* 2006, 177: 7059–7066.

The parasite *Trypanosoma cruzi* is an intracellular protozoan that causes Chagas' disease, a chronic systemic disorder affecting nearly 20 million people in Central and South America. Host defense against *T. cruzi* depends on a variety of cell populations, including NK, CD4$^+$ T cells, CD8$^+$ T cells, and Ig-producing B cells (1–3). In addition, macrophages and dendritic cells (DCs)[3] produce proinflammatory cytokines, such as IL-12, in response to invasion by *T. cruzi* (4–6). IL-12 induces IFN-γ production by NK, CD4$^+$ T cells, and CD8$^+$ T cells. In turn, IFN-γ induces NO production by macrophages and mediates the killing of *T. cruzi* (7, 8). This cytokine milieu is therefore responsible for host resistance to *T. cruzi* infection in vivo. However, it remains uncertain how innate immune cells, such as macrophages and DCs, mediate *T. cruzi*-induced immune responses during the early phase of infection. In addition, *T. cruzi* infection induces the production of type I IFNs (αβ IFN), which possess antiviral activities (9, 10). However, the nature of the involvement of type I IFNs in response to *T. cruzi* infection remains controversial (11).

A family of TLRs has been identified that recognize specific components of various microorganisms, including bacteria, viruses, fungi, and protozoan parasites (12). Recognition of microbial components by TLRs triggers the activation of innate immunity and the subsequent development of Ag-specific adaptive immunity. TLR-mediated signaling pathways originate from the cytoplasmic Toll/IL-1R (TIR) domains, which are conserved among all family members. A group of TIR domain-containing adaptors (MyD88, Toll/IL-1R domain-containing adaptor protein, TIR domain-containing adaptor-inducing IFN-β (TRIF), and TRIF-related adaptor molecule) have been shown to be integral to these TLR signaling pathways (13). The TLR signaling pathways consist of two cascades: a MyD88-dependent pathway and a TRIF-dependent (MyD88-independent) pathway. The MyD88-dependent pathway mediates all TLR-induced productions of proinflammatory cytokines, including IL-12p40, whereas the TRIF-dependent pathway is indispensable for the induction of type I IFNs through TLR3 and TLR4.

Previous studies have analyzed the involvement of TLR-dependent activation of innate immunity in *T. cruzi* infection. TLR2, TLR4, and TLR9 have been implicated in the recognition of *T. cruzi*-derived components (6, 14–16), whereas mice lacking MyD88 were found to be susceptible to the acute phase of *T. cruzi* infection accompanied by defective proinflammatory cytokine production (17). However, even in MyD88-deficient mice, significant IFN-γ production was still observed, indicating the presence of MyD88-independent immune responses. Thus, the nature of the involvement of innate immunity in *T. cruzi* infection still remains to be precisely characterized.

In the present study, we analyzed the involvement of innate immune cells in *T. cruzi* infection using mice lacking both

*Department of Molecular Genetics, Medical Institute of Bioregulation and †Department of Parasitology, Faculty of Medical Sciences, Kyushu University, Fukuoka, Japan; and ‡Department of Host Defense, Institute for Microbial Diseases, Osaka University, and Exploratory Research for Advanced Technology, Japan Science and Technology Agency, Suita, Japan

Received for publication May 31, 2006. Accepted for publication September 1, 2006.

The costs of publication of this article were defrayed in part by the payment of page charges. This article must therefore be hereby marked *advertisement* in accordance with 18 U.S.C. Section 1734 solely to indicate this fact.

[1] This work was supported by grants from the Special Coordination Funds of the Ministry of Education, Culture, Sports, Science and Technology, as well as the Uehara Memorial Foundation, the Mitsubishi Foundation, the Takeda Science Foundation, the Tokyo Biochemical Research Foundation, the Kowa Life Science Foundation, the Osaka Foundation for Promotion of Clinical Immunology, and the Sankyo Foundation of Life Science.

[2] Address correspondence and reprint requests to Dr. Kiyoshi Takeda, Department of Molecular Genetics, Medical Institute of Bioregulation, Kyushu University, 3-1-1 Maidashi, Higashi-ku, Fukuoka 812-8582, Japan. E-mail address: ktakeda@bioreg.kyushu-u.ac.jp

[3] Abbreviations used in this paper: DC, dendritic cell; TIR, Toll/IL-1R; TRIF, TIR domain-containing adaptor-inducing IFN-β; WT, wild type; siRNA, small interfering RNA; EF-1α, elongation factor-1α.

0022-1767/06/$02.00

MyD88 and TRIF, in which all of the previously described TLR-mediated activation mechanisms of innate immunity are totally abolished.

Materials and Methods

Mice

MyD88$^{-/-}$ and TRIF$^{-/-}$ mice were generated as previously described (18, 19). Type I IFN receptor (IFNAR1)$^{-/-}$ mice were purchased from B & K Universal (20). Each mouse strain was backcrossed to C57BL/6 for at least five generations, and then used to generate double-mutant mice. MyD88$^{-/-}$TRIF$^{-/-}$ mice were generated by crossing MyD88$^{+/-}$ TRIF$^{+/-}$ mice. Littermate wild-type (WT) (MyD88$^{+/-}$TRIF$^{+/-}$), MyD88$^{-/-}$ (MyD88$^{-/-}$TRIF$^{+/-}$), and TRIF$^{-/-}$ (MyD88$^{+/-}$TRIF$^{-/-}$) mice were used for the experiments. MyD88$^{-/-}$IFNAR1$^{-/-}$ mice were generated by crossing MyD88$^{+/-}$IFNAR1$^{+/-}$ mice, and used for the experiments at 8–10 wk of age. All animal experiments were conducted in accordance with the guidelines of the Animal Care and Use Committee of Kyushu University.

Preparation of macrophages and DCs

To isolate peritoneal macrophages, mice were i.p. injected with 2 ml of 4% thioglycolate medium (Sigma-Aldrich), and peritoneal exudate cells were isolated from the peritoneal cavity at 3 days postinjection. The cells were incubated for 2 h and washed three times with HBSS. The remaining adherent cells were used as peritoneal macrophages in experiments. To prepare bone marrow-derived DCs or macrophages, bone marrow cells were prepared from the femur and tibia, passed through a nylon mesh and cultured in RPMI 1640 medium supplemented with 10% FBS, 100 mM 2-ME, and 10 ng/ml GM-CSF (PeproTech) or 30% L cell culture supernatant. After 6 days, the cells were used as DCs or macrophages in experiments.

Parasites and experimental infection

The *T. cruzi* Tulahuén strain was maintained in vivo in IFN-γR$^{-/-}$ mice by passages every other week (21). For in vitro experiments, macrophages or DCs (5×10^4) were infected with 5×10^4 trypomastigotes. After 6 h of infection, the cells were washed twice with PBS to remove the extracellular parasites and cultured in RPMI 1640 supplemented with 10% FBS for the indicated time periods. Trypomastigotes in the culture supernatants were counted microscopically. Alternatively, the cells were pulsed with 1 μCi of [^{3}H]uracil and cultured for 72 h. The cells were then harvested on glass fiber filters and the incorporated uracil was measured using a liquid scintillation counter. The net cpm was calculated by subtracting the background cpm in uninfected cultures from the cpm of the infected cultures. In some experiments, macrophages were infected with *T. cruzi* in the absence or presence of 10 ng/ml of an anti-IFN-β neutralizing Ab (YAMASA) for 6 h, washed and then further cultured with or without the anti-IFN-β Ab.

In other experiments, extracellular parasites were removed by repeated washing after 6h of infection, and the cells were incubated for a further 48 h. Subsequently, the cells were washed, fixed and stained using a Diff-Quik kit (Sysmex). The intracellular parasite numbers in 250 macrophages were counted under a light microscope. Counting was performed in a blinded manner by two independent investigators.

For in vivo experiments, mice were i.p. injected with plasma containing 2×10^3 or 1×10^4 trypomastigotes as indicated. The number of parasites in the blood of each animal was then counted microscopically using 5 μl of blood taken from the tail. Statistical significance was determined using a paired Student's *t* test. Differences were considered to be statistically significant at $p < 0.05$.

Measurement of cytokine production

Peritoneal macrophages or DCs (5×10^4) were infected with 5×10^4 *T. cruzi* for 6 h, extensively washed and cultured for 24 h. The culture supernatants were collected and analyzed for their levels of TNF-α by ELISA (Genzyme Techne) and NO using the Griess reagent (Dojindo Laboratories).

Quantitative real-time RT-PCR

Total RNA was isolated with an RNeasy mini kit (Qiagen), and 2 μg of the RNA was reverse-transcribed using M-MLV reverse transcriptase (Promega) and oligo(dT) primers (Toyobo) after treatment with RQ1 DNase I (Promega). Quantitative real-time PCR was performed in an ABI 7000 (Applied Biosystems) using TaqMan Universal PCR Master Mix (Applied Biosystems). All data were normalized to the corresponding level of elongation factor-1α (EF-1α) expression, and the fold difference relative to the EF-1α level was calculated. The amplification conditions were: 50°C (2 min), 95°C (10 min), and 40 cycles of 95°C (15 s), and 60°C (60 s). Each experiment was performed independently at least three times, and the results of one representative experiment are shown. All primers were purchased from Assay on Demand (Applied Biosystems).

RNA interference

For small interfering RNA (siRNA) experiments, dsRNA duplexes targeting the coding region of the GTPase IFN-inducible p47 (IRG47) (5′-GGUGGAUAGUGACUUAUAUtt-3′) were synthesized by Ambion. Bone marrow cells were cultured in the presence of 30% L cell culture supernatant for 6 days. The differentiated bone marrow macrophages were then harvested by 5 mM EDTA treatment and transfected with 1.5 μg of the siRNA using Nucleofector and a Mouse Macrophage Nucleofector kit (Amaxa Biosystems) according to the manufacturer's instructions. The cells were immediately transferred to culture medium and cultured for 18 h. Next, cells were infected with *T. cruzi* for 48 h, and parasite growth was analyzed. To determine the efficiency of gene silencing, cells were infected with *T. cruzi* for 6 h, and the expression of IRG47 mRNA was analyzed by quantitative real-time RT-PCR.

Results

Increased growth of T. cruzi *in MyD88$^{-/-}$TRIF$^{-/-}$ DCs and macrophages*

To study the direct involvement of innate immunity in *T. cruzi* infection, bone marrow-derived DCs prepared from WT, MyD88$^{-/-}$, TRIF$^{-/-}$, or MyD88$^{-/-}$TRIF$^{-/-}$ mice were infected with *T. cruzi*. After 6 h of *T. cruzi* infection, the cells were extensively washed and changed to fresh medium. After culture periods of 4, 5, and 7 days, the number of trypomastigotes released into the culture supernatants were counted (Fig. 1*A*). The culture supernatant of TRIF$^{-/-}$ DCs contained a similar number of trypomastigotes to that of WT DCs. For MyD88$^{-/-}$ DCs, the number of trypomastigotes increased after 5 and 7 days of infection. Furthermore, for MyD88$^{-/-}$TRIF$^{-/-}$ DCs, the number of trypomastigotes increased considerably. Next, peritoneal macrophages were infected with *T. cruzi* (Fig. 1*B*). The number of trypomastigotes in the culture supernatant of MyD88$^{-/-}$ macrophages was slightly increased compared with those of WT or TRIF$^{-/-}$ cells after 5 and 7 days of infection. For MyD88$^{-/-}$TRIF$^{-/-}$ macrophages, larger numbers of trypomastigotes were observed compared with the other cell genotypes after 7 days of infection. Next, replication of *T. cruzi* within macrophages was assessed based on [^{3}H]uracil incorporation (Fig. 1*C*). Intracellular growth of *T. cruzi* was slightly increased in MyD88$^{-/-}$ macrophages, and markedly increased in MyD88$^{-/-}$TRIF$^{-/-}$ cells compared with WT cells. Bone marrow-derived macrophages were also infected with *T. cruzi* and cultured for 48 h, before the number of intracellular parasites was counted. The number of infected cells did not differ among the genotypes (data not shown). However, infected MyD88$^{-/-}$TRIF$^{-/-}$ macrophages contained an increased number of parasites after 48 h of infection (Fig. 1, *D* and *E*). Thus MyD88$^{-/-}$ DCs and macrophages showed a slight increase in *T. cruzi* growth, whereas MyD88$^{-/-}$TRIF$^{-/-}$ cells showed a marked increase in growth, indicating that MyD88$^{-/-}$TRIF$^{-/-}$ DCs and macrophages were defective in the clearance of *T. cruzi*.

Defective T. cruzi *induction of proinflammatory mediators in MyD88$^{-/-}$ macrophages and DCs*

The killing of parasites by macrophages has been shown to be mediated by TNF-α and NO (22–25). Therefore, we next analyzed the production of TNF-α and NO by *T. cruzi*-infected peritoneal macrophages (Fig. 2). Both WT and TRIF$^{-/-}$ macrophages secreted TNF-α and NO in response to *T. cruzi* infection. In contrast,

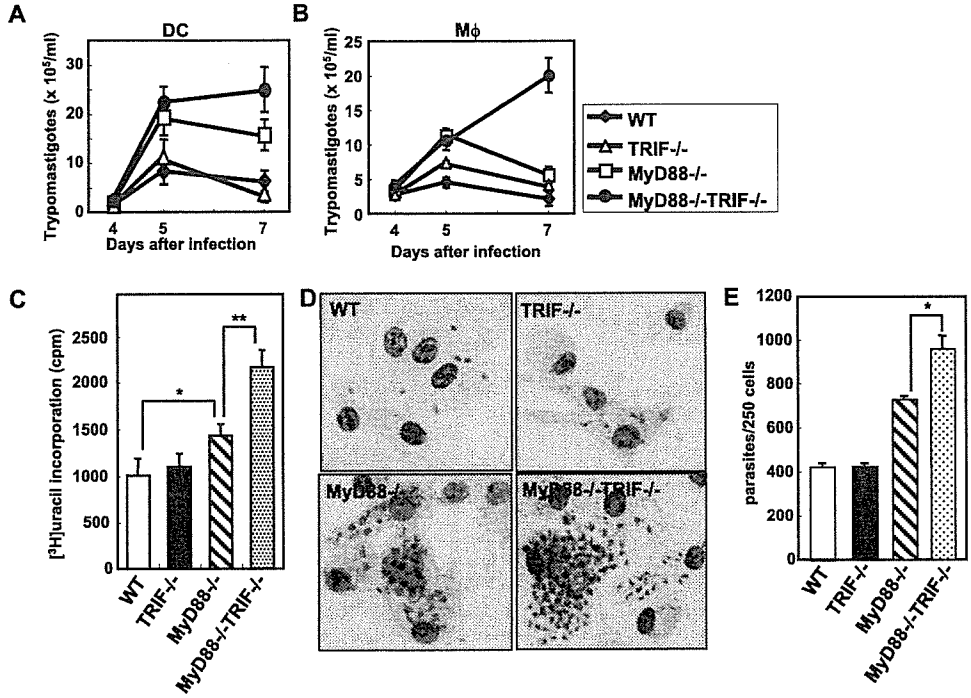

FIGURE 1. Defective *T. cruzi* clearance in MyD88$^{-/-}$TRIF$^{-/-}$ DCs and macrophages. Bone marrow-derived DCs (*A*) or peritoneal macrophages (Mϕ) (*B*) from WT, TRIF$^{-/-}$, MyD88$^{-/-}$, or MyD88$^{-/-}$TRIF$^{-/-}$ mice were seeded onto 96-well plates, and infected with *T. cruzi* for 6 h. The cells were then washed to remove the extracellular parasites and cultured for the indicated periods, before the numbers of trypomastigotes in the culture supernatants were counted. Data are representative of four independent experiments. *C*, Peritoneal macrophages were infected with *T. cruzi*, washed and cultured in the presence of [^{3}H]uracil for 72 h, before the [^{3}H]uracil incorporation was measured. *, $p < 0.01$; **, $p < 0.005$. *D* and *E*, Bone marrow-derived macrophages were infected with *T. cruzi*, washed, and cultured for 48 h. The cells were then fixed, stained, and analyzed by microscopy. Representative stained cells from three independent experiments are shown. Magnification, ×400. The intracellular parasites were counted, and the data represent the mean + SD of the number of parasites per 250 macrophages. *, $p < 0.02$.

secretion of these mediators was severely reduced in both MyD88$^{-/-}$ and MyD88$^{-/-}$TRIF$^{-/-}$ macrophages, and no significant differences were observed between the two genotypes. These findings indicate that *T. cruzi*-induced production of TNF-α and NO was dependent on MyD88, but that the higher susceptibility to *T. cruzi* infection of MyD88$^{-/-}$TRIF$^{-/-}$ macrophages was not due to defective induction of these mediators.

Defective T. cruzi *induction of IFN-inducible genes in MyD88$^{-/-}$TRIF$^{-/-}$ macrophages and DCs*

Next, we tried to identify which genes were selectively less active in *T. cruzi*-infected MyD88$^{-/-}$TRIF$^{-/-}$ DCs. *T. cruzi* infection has been shown to induce IFN-β (9, 10). Therefore, we analyzed *T. cruzi*-induced gene expression focusing on IFN-β and IFN-inducible chemokines as well as proinflammatory cytokines in peritoneal macrophages and DCs from WT, TRIF$^{-/-}$, MyD88$^{-/-}$, and MyD88$^{-/-}$TRIF$^{-/-}$ mice by quantitative real-time RT-PCR. In WT and TRIF$^{-/-}$ macrophages, *T. cruzi* infection led to robust induction of TNF-α and IL-12p40 mRNAs (Fig. 3*A*). In contrast, both MyD88$^{-/-}$ and MyD88$^{-/-}$TRIF$^{-/-}$ macrophages showed defective induction of TNF-α and IL-12p40. Expression of the mRNAs for IFN-β and IFN-inducible genes, such as *Ccl2* (MCP-1), *Ccl5* (RANTES), and *Cxcl10* (IP-10) was induced in *T. cruzi*-infected WT DCs (Fig. 3*B*). In contrast, *T. cruzi*-induced expression of IFN-α4 mRNA was not observed in any of the macrophage and DC genotypes (data not shown). In MyD88$^{-/-}$ DCs, *T. cruzi*-induced expression of *Ccl2*, *Ccl5*, and *Cxcl10* was only slightly reduced. However, DCs from TRIF$^{-/-}$ and MyD88$^{-/-}$TRIF$^{-/-}$ mice showed severely impaired induction of these genes after *T. cruzi* infection. Peritoneal macrophages from each genotype showed similar patterns of *T. cruzi*-induced gene expression (Fig. 3*C*). Thus, MyD88$^{-/-}$ macrophages and DCs showed defective induction of proinflammatory cytokine genes during *T. cruzi* infection, whereas TRIF$^{-/-}$ cells showed defective induction of IFN-β and IFN-inducible genes during the infection. Furthermore, MyD88$^{-/-}$TRIF$^{-/-}$ cells displayed defective expression of all these genes.

IFN-β-mediated inhibition of T. cruzi *growth in MyD88$^{-/-}$ macrophages*

MyD88$^{-/-}$TRIF$^{-/-}$ macrophages and DCs displayed defective clearance of *T. cruzi* with impaired expression of IFN-β and IFN-inducible genes. Therefore, we next addressed whether IFN-β is involved in the resistance to *T. cruzi* infection in MyD88$^{-/-}$ macrophages. Peritoneal macrophages from WT and MyD88$^{-/-}$ mice were infected with *T. cruzi* in the presence of an anti-IFN-β neutralizing Ab, and intracellular growth of *T. cruzi* was measured (Fig. 4). In WT macrophages, *T. cruzi* growth remained unaltered by the addition of the anti-IFN-β Ab. In contrast, anti-IFN-β Ab addition dramatically increased the intracellular growth of *T. cruzi* in MyD88$^{-/-}$ macrophages. These findings indicate the possible involvement of IFN-β in resistance to *T. cruzi* infection in the absence of MyD88.

High-sensitivity to T. cruzi *infection in MyD88$^{-/-}$IFNAR1$^{-/-}$ macrophages*

To further address whether IFN-β is involved in the resistance to *T. cruzi* infection, we generated mice lacking both MyD88 and the IFNAR1 subunit of the $\alpha\beta$ IFN receptor complex (MyD88$^{-/-}$ IFNAR1$^{-/-}$ mice). Bone marrow-derived macrophages were infected with *T. cruzi*, washed, and cultured. After culture periods of 4, 5, and 7 days, the numbers of trypomastigotes in the culture

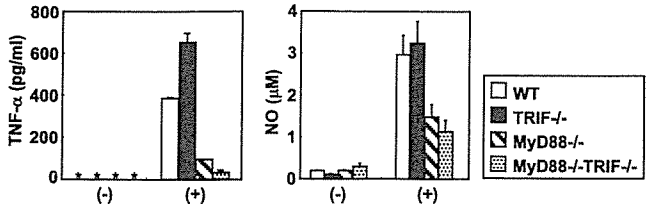

FIGURE 2. Defective production of TNF-α and NO in *T. cruzi*-infected MyD88$^{-/-}$ macrophages. Peritoneal macrophages from WT, TRIF$^{-/-}$, MyD88$^{-/-}$, or MyD88$^{-/-}$TRIF$^{-/-}$ mice were infected with (+) or without (−) *T. cruzi* for 6 h, washed to remove the extracellular parasites, and cultured for 24 h. The levels of TNF-α and NO in the culture supernatants were measured. *, Not detected.

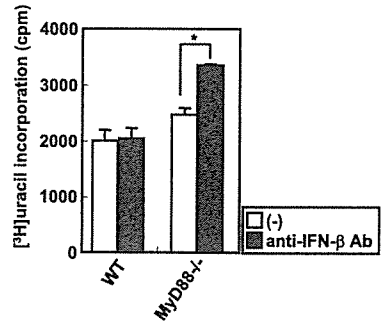

FIGURE 4. Effect of an anti-IFN-β neutralizing Ab on *T. cruzi* growth in macrophages. Peritoneal macrophages from WT or MyD88$^{-/-}$ mice were infected with *T. cruzi* for 6 h in the presence or absence of an anti-IFN-β neutralizing Ab, washed, and cultured in the presence of [^{3}H]uracil for 72 h. The [^{3}H]uracil incorporation was then measured. *, $p < 0.005$.

supernatants were counted (Fig. 5*A*). As mentioned, the culture supernatant of MyD88$^{-/-}$ macrophages contained a larger number of trypomastigotes than that of WT macrophages. In the supernatant of IFNAR1$^{-/-}$ macrophages, a slight increase in the number of trypomastigotes was observed compared with WT cells. Furthermore, the number of trypomastigotes in the culture supernatant of MyD88$^{-/-}$IFNAR1$^{-/-}$ macrophages was considerably increased. Next, intracellular replication of *T. cruzi* was assessed by counting [^{3}H]uracil incorporation (Fig. 5*B*). MyD88$^{-/-}$ and IFNAR1$^{-/-}$ macrophages showed slightly increased growth rates of *T. cruzi*. However, MyD88$^{-/-}$IFNAR1$^{-/-}$ macrophages showed markedly increased growth rates of *T. cruzi* compared with MyD88$^{-/-}$ or IFNAR1$^{-/-}$ cells. Furthermore, at 48 h after the *T. cruzi* infection, increased numbers of parasites were observed in MyD88$^{-/-}$IFNAR1$^{-/-}$ macrophages (Fig. 5, *C* and *D*). Thus, IFNAR1$^{-/-}$ macrophages displayed a slightly increased sensitivity to *T. cruzi* infection, whereas MyD88$^{-/-}$IFNAR1$^{-/-}$ macrophages displayed a higher sensitivity to the infection. These findings suggest that IFN-β is responsible for resistance to *T. cruzi* infection and that this responsibility becomes evident in the absence of MyD88.

High-sensitivity MyD88$^{-/-}$IFNAR1$^{-/-}$ mice to T. cruzi *infection*

Macrophages are the primary site of *T. cruzi* replication, and thus act as the major cell population for controlling the infection in vivo, especially for reticulotropic strains such as the Tulahuén strain used in the present study (21, 26). Therefore, we next addressed whether IFN-β mediates antitrypanosomal responses in vivo. Mice were i.p. infected with *T. cruzi*, and the parasitemia was monitored (Fig. 6*A*). In WT and TRIF$^{-/-}$ mice, the trypomastigote counts in the sera peaked by day 13 of the infection, and subsequently decreased. In IFNAR1$^{-/-}$ mice, serum trypomastigotes were slightly increased compared with WT or TRIF$^{-/-}$ mice, and peaked around 11–13 days of infection. In MyD88$^{-/-}$ mice, the parasite counts were increased at 13 days of infection. In MyD88$^{-/-}$ TRIF$^{-/-}$ mice, the serum parasite counts continued to increase, and these mice showed much higher levels of parasitemia by day 15 of infection than levels found in MyD88$^{-/-}$ mice. In MyD88$^{-/-}$ IFNAR1$^{-/-}$ mice, the parasite counts increased in a similar manner

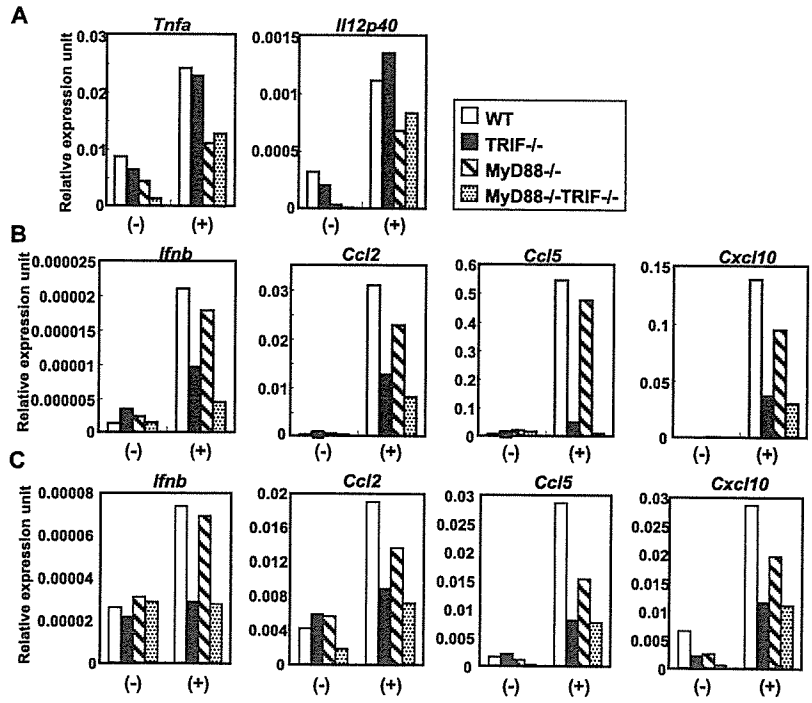

FIGURE 3. *T. cruzi*-induced expression of inflammatory genes in macrophages and DCs. *A*, Peritoneal macrophages from WT, TRIF$^{-/-}$, MyD88$^{-/-}$, or MyD88$^{-/-}$TRIF$^{-/-}$ mice were cultured in the presence (+) or absence (−) of *T. cruzi* for 6 h. Total RNA was then extracted and analyzed for the expressions of *Tnfa* or *Il-12p40* by quantitative real-time RT-PCR. The data are shown as the relative mRNA levels normalized by the corresponding EF-1α mRNA level. Bone marrow-derived DCs (*B*) or peritoneal macrophages (*C*) from WT, TRIF$^{-/-}$, MyD88$^{-/-}$, or MyD88$^{-/-}$TRIF$^{-/-}$ mice were cultured in the presence (+) or absence (−) of *T. cruzi* for 6 h. Total RNA was then extracted and analyzed for the expressions of *Ifnb*, *Ccl2*, *Ccl5*, and *Cxcl10* by quantitative real-time RT-PCR. Data are presented in relative expression units and have been normalized to the corresponding EF-1α mRNA level.

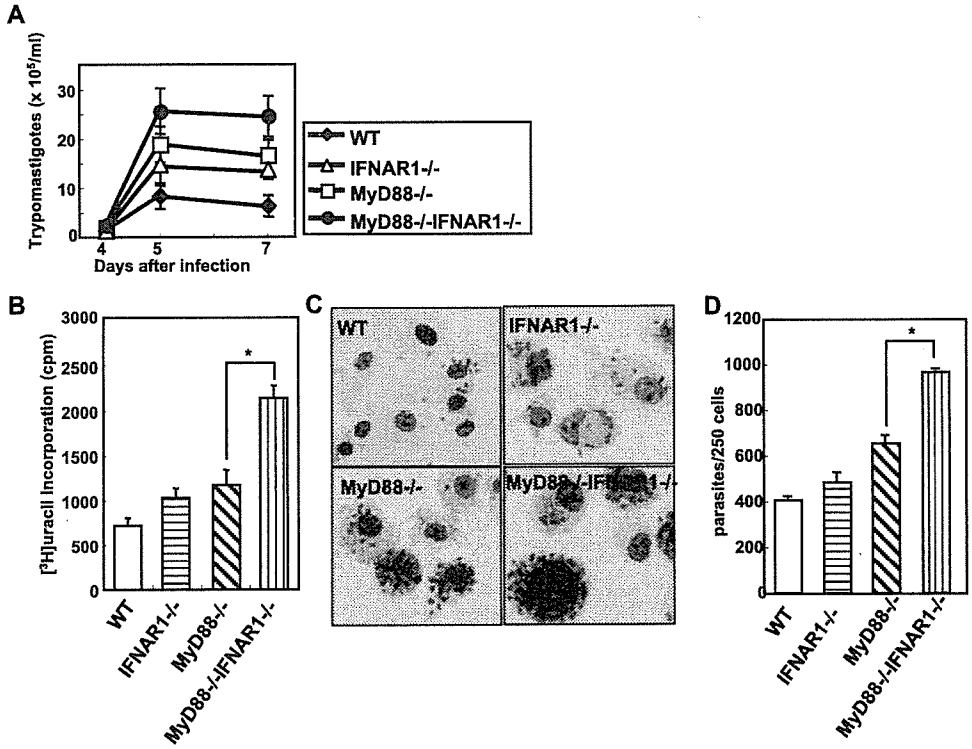

FIGURE 5. Increased *T. cruzi* growth in MyD88$^{-/-}$IFNAR1$^{-/-}$ macrophages. *A*, Bone marrow-derived macrophages from WT, MyD88$^{-/-}$, IFNAR1$^{-/-}$, or MyD88$^{-/-}$IFNAR1$^{-/-}$ mice were infected with *T. cruzi* for 6 h, washed to remove the extracellular parasites, and cultured for the indicated periods. The trypomastigotes in the culture supernatants were counted. Data are representative of four independent experiments. *B*, Peritoneal macrophages were infected with *T. cruzi*, washed, and cultured in the presence of [^{3}H]uracil for 72 h. The [^{3}H]uracil incorporation was then measured. *, $p < 0.0001$. *C* and *D*, Bone marrow-derived macrophages from each genotype were infected with *T. cruzi*, washed, and cultured for 48 h. The cells were then fixed, stained, and analyzed by microscopy. Representative stained cells from three independent experiments are shown. Magnification, ×400. Intracellular parasites were counted, and the data represent the mean + SD of the number of parasites per 250 macrophages. *, $p < 0.02$.

to those in MyD88$^{-/-}$TRIF$^{-/-}$ mice. We further monitored the mortality of the mice after *T. cruzi* infection (Fig. 6*B*). WT, TRIF$^{-/-}$, and IFNAR1$^{-/-}$ mice were resistant to *T. cruzi* infection, and all the mice survived for more than 19 days after the infection, whereas MyD88$^{-/-}$ mice started to die around 15 days after the infection, and about half of the mice had died within 19 days. In contrast, all the MyD88$^{-/-}$TRIF$^{-/-}$ and MyD88$^{-/-}$IFNAR1$^{-/-}$ mice died within 19 days of the infection. Thus, MyD88$^{-/-}$TRIF$^{-/-}$ and MyD88$^{-/-}$IFNAR1$^{-/-}$ mice were more sensitive to in vivo *T. cruzi* infection than MyD88$^{-/-}$ mice, suggesting that IFN-β mediates in vivo resistance to *T. cruzi* infection, and this effect becomes evident in the absence of MyD88.

Involvement of IFN-β-inducible IRG47 in resistance to T. cruzi *infection*

Next, we addressed the molecular mechanisms of the IFN-β-mediated resistance to *T. cruzi* infection in innate immune cells. The family of p47 GTPases has been shown to control innate immune responses to intracellular pathogens, including protozoan parasites (27, 28). In addition, expression of p47 GTPases, such as LRG47

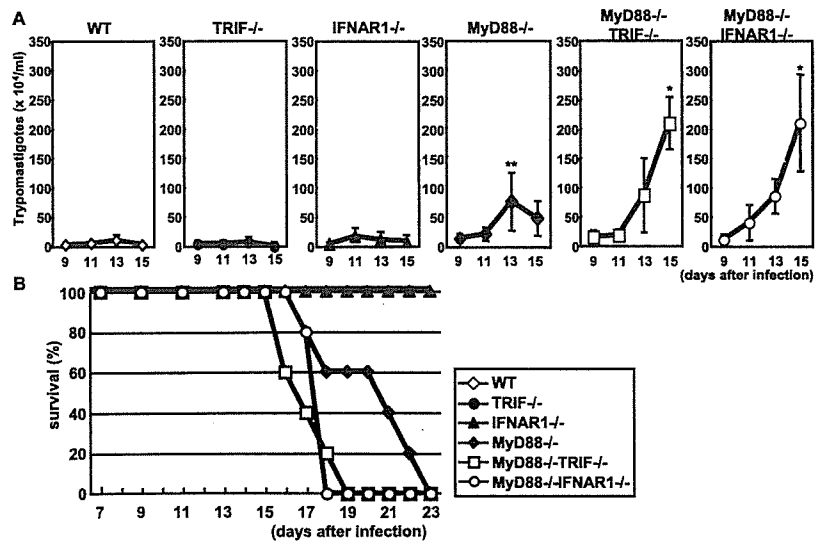

FIGURE 6. High-sensitivity MyD88$^{-/-}$IFNAR1$^{-/-}$ mice to *T. cruzi* infection. WT (n = 9), TRIF$^{-/-}$ (n = 10), IFNAR1$^{-/-}$ (n = 10), MyD88$^{-/-}$ (n = 5), MyD88$^{-/-}$TRIF$^{-/-}$ (n = 5), and MyD88$^{-/-}$IFNAR1$^{-/-}$ (n = 5) mice were i.p. infected with 1×10^4 *T. cruzi*. Parasitemia (*A*) and mortality (*B*) were monitored at the indicated times after infection. *, $p < 0.001$ compared with MyD88$^{-/-}$ mice and **, $p < 0.005$ compared with control mice.

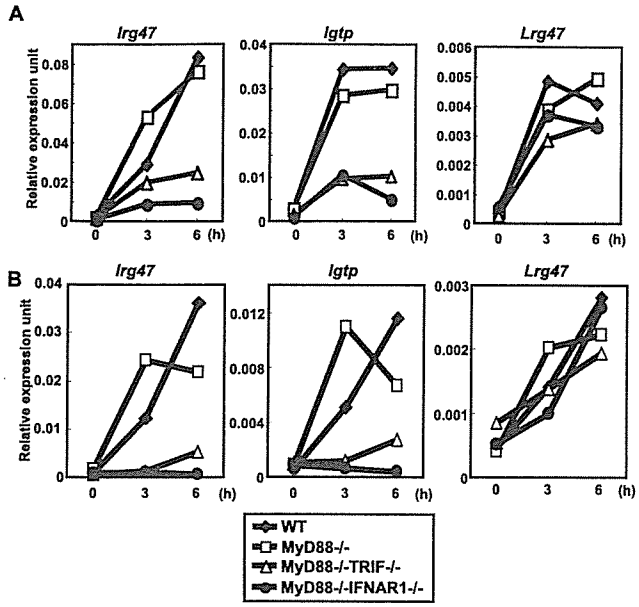

FIGURE 7. Impaired expression of IRG47 in *T. cruzi*-infected MyD88$^{-/-}$TRIF$^{-/-}$ mice. Bone marrow-derived macrophages (*A*) or DCs (*B*) from WT, MyD88$^{-/-}$, MyD88$^{-/-}$TRIF$^{-/-}$, or MyD88$^{-/-}$IFNAR1$^{-/-}$ mice were infected with *T. cruzi* for 3 or 6 h. Next, total RNA was extracted and analyzed for the expressions of *Irg47*, *Igtp*, *and Lrg47* by quantitative real-time RT-PCR. Data are shown as the relative mRNA levels normalized to the corresponding EF-1α mRNA level.

and IRG47, and inducibly expressed GTPase (IGTP), has been shown to be induced through activation of TLR and IFN signaling pathways during infection with intracellular pathogens (27, 28). Therefore, we analyzed the expression levels of these p47 GTPases in *T. cruzi*-infected DCs and macrophages. Bone marrow-derived macrophages or DCs from WT, MyD88$^{-/-}$, MyD88$^{-/-}$TRIF$^{-/-}$, and MyD88$^{-/-}$IFNAR1$^{-/-}$ mice were infected with *T. cruzi* for 3 or 6 h, and the expression of LRG47, IRG47, and IGTP mRNAs was analyzed (Fig. 7, *A* and *B*). In WT and MyD88$^{-/-}$ macrophages and DCs, *T. cruzi* infection resulted in robust mRNA expressions of all these p47 GTPases. Even in MyD88$^{-/-}$TRIF$^{-/-}$ and MyD88$^{-/-}$IFNAR1$^{-/-}$ cells, almost normal *T. cruzi*-induced expression of LRG47 mRNA was observed. However, *T. cruzi*-induced expression of IRG47 and IGTP mRNAs was severely impaired in MyD88$^{-/-}$TRIF$^{-/-}$ and MyD88$^{-/-}$IFNAR1$^{-/-}$ macrophages and DCs. Although IGTP was previously shown to have a minor role in *T. cruzi* infection, the involvement of IRG47 in *T. cruzi* infection is less well defined (29). Therefore, we next analyzed whether IRG47 is responsible for antitrypanosomal responses in the absence of MyD88. To complete this analysis, siRNA-mediated knockdown of IRG47 was performed in MyD88$^{-/-}$ macrophages. We transfected an IRG47 or control siRNA into bone marrow-derived macrophages and extracted the total RNA after 18 h for analysis of the IRG47 expression (Fig. 8*A*). Introduction of the IRG47 siRNA into bone marrow-derived macrophages from MyD88$^{-/-}$ mice resulted in an effective (81%) reduction in IRG47 mRNA expression. MyD88$^{-/-}$ macrophages transfected with the IRG47 or control siRNA were further infected with *T. cruzi*, and the intracellular parasites were visualized and counted (Fig. 8, *B* and *C*). In MyD88$^{-/-}$ macrophages, siRNA-mediated knockdown of IRG47 led to increased numbers of intracellular *T. cruzi*. These results indicate that IRG47 is involved in resistance to *T. cruzi* infection in innate immune cells.

Discussion

In the present study, we analyzed innate immune responses to the intracellular protozoan parasite *T. cruzi* using MyD88$^{-/-}$TRIF$^{-/-}$ mice, in which TLR-dependent activation of innate immunity is not induced. Macrophages and DCs derived from MyD88$^{-/-}$TRIF$^{-/-}$ mice showed impaired clearance of *T. cruzi*. Analysis of the gene expression profiles of *T. cruzi*-infected MyD88$^{-/-}$TRIF$^{-/-}$ DCs revealed that IFN-β was induced in a TRIF-dependent manner during *T. cruzi* infection, whereas analyses with an anti-IFN-β neutralizing Ab and MyD88$^{-/-}$IFNAR1$^{-/-}$ cells demonstrated that IFN-β mediated antitrypanosomal innate immune responses. Furthermore, both MyD88$^{-/-}$TRIF$^{-/-}$ and MyD88$^{-/-}$IFNAR1$^{-/-}$ mice were highly sensitive to in vivo *T. cruzi* infection. These findings indicate that MyD88-dependent induction of proinflammatory cytokines and TRIF-dependent induction of IFN-β both contribute to innate immune responses to *T. cruzi* infection. We further showed that the p47 GTPase IRG47 is responsible for the resistance to *T. cruzi* infection in MyD88$^{-/-}$ macrophages.

Type I IFNs are well-known cytokines that exhibit antiviral activities (30). However, a large body of evidence has demonstrated

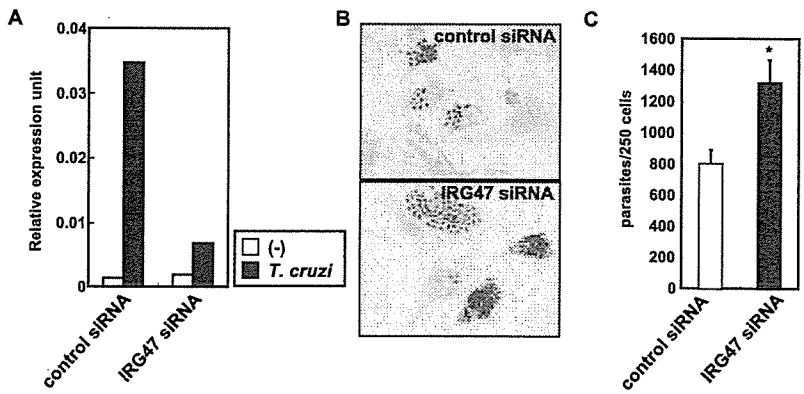

FIGURE 8. IRG47 mediates antitrypanosomal activity in MyD88$^{-/-}$ mice. *A*, Bone marrow-derived macrophages were transfected with IRG47 or control siRNA and cultured for 18 h. The cells were then infected with *T. cruzi* for 6 h and analyzed for the expression of IRG47 mRNA by quantitative real-time RT-PCR. Data are shown as the relative mRNA levels normalized to the corresponding EF-1α mRNA level. *B* and *C*, Bone marrow-derived macrophages transfected with an IRG47 or control siRNA were infected with *T. cruzi*, washed, and cultured for 48 h. The cells were then fixed, stained, and analyzed by microscopy. Representative stained cells from three independent experiments are shown. Magnification, ×400. Intracellular parasites were counted, and the data represent the mean + SD of the number of parasites per 250 macrophages. *, $p < 0.02$ compared with control siRNA-transfected cells.

that type I IFNs are also induced by nonviral pathogens, such as bacteria, mycobacteria, and protozoan parasites (11, 31). In the case of bacterial infection, type I IFNs seem to have opposing effects depending on the type of bacteria (31). Although exogenous type I IFNs show protective actions in response to infection with *Salmonella typhimurium* or *Shigella flexneri*, the protective effects of endogenous type I IFNs remain unclear (32, 33). In contrast, endogenous type I IFNs reduce resistance to *Listeria monocytogenes* infection (34–36). During infection with the protozoan parasite *Leishmania major*, these exogenous IFNs presumably have a protective effect through the induction of inducible NO synthase, although the involvement of endogenous type I IFNs in antileishmanial immunity is less clear (37, 38). Following infection with *T. cruzi*, administration of exogenous $\alpha\beta$ IFN was reported to reduce the number of serum parasites (10). However, a subsequent study showed that IFNAR1$^{-/-}$ mice were not susceptible to the infection, indicating that endogenous $\alpha\beta$ IFN do not contribute to the host defense against *T. cruzi* (39). Thus, the possible roles of type I IFNs in antitrypanosomal immune responses remain controversial. In the present study, we have clearly established that IFN-β produced by DCs and macrophages contributes to host defense against *T. cruzi*. Thus, endogenous type I IFNs produced during *T. cruzi* infection are responsible for antitrypanosomal immune responses, although the MyD88-dependent production of proinflammatory cytokines overshadows the effects of type I IFNs in normal mice. In the future, it will be interesting to investigate whether this mechanism also applies to immune responses to other protozoan parasites, such as *L. major* and *Toxoplasma gondii*.

We further analyzed the mechanisms by which IFN-β exerts antitrypanosomal responses. The p47 GTPase family members control innate immune responses to intracellular pathogens, including protozoan parasites (27, 28). Expression of p47 GTPases, such as LRG47 and IRG47, and of IGTP is induced through the activation of TLR and IFN signaling pathways during infection with intracellular pathogens. Mice lacking LRG47, IRG47, or IGTP have been shown to become sensitive to infection with *L. major* and *T. gondii*, indicating the possible involvement of these GTPases in *T. cruzi* infection (27, 40, 41). Indeed, LRG47-deficient mice have recently been shown to be sensitive to *T. cruzi* infection (42). We found that induction of IRG47 was impaired in *T. cruzi*-infected cells from MyD88$^{-/-}$TRIF$^{-/-}$ and MyD88$^{-/-}$IFNAR1$^{-/-}$ mice. Knockdown of IRG47 in MyD88$^{-/-}$ macrophages led to increased intracellular parasites. Thus, TLR-dependent expression of IFN-β probably mediates antitrypanosomal responses through the induction of IRG47.

Recently, MyD88$^{-/-}$TRIF$^{-/-}$ macrophages have been shown to produce IFN-β when infected with intracellular pathogens that escape into the cytosol, such as *L. monocytogenes* and *Legionella pneumophila* (43). In contrast, *T. cruzi*-induced IFN-β production was not observed in MyD88$^{-/-}$TRIF$^{-/-}$ macrophages, although this parasite also invades the cytosol (44). In the case of the cytosolic escape of *Listeria* or *Legionella*, dsDNA from the bacteria is responsible for the induction of IFN-β (43, 45). In contrast to these prokaryotic bacteria, *T. cruzi* is a eukaryote. Therefore, it seems less likely that trypanosomal DNA within the nucleus is exposed to the host cell cytosol, which may lead to the observed absence of TLR-independent induction of IFN-β. Thus, recognition of *T. cruzi* invasion is mainly dependent on TLR systems, possibly at the plasma membrane or in the phagolysosome. However, even in MyD88$^{-/-}$TRIF$^{-/-}$ macrophages, the gene encoding LRG47 was induced after *T. cruzi* infection, indicating the presence of TLR-independent mechanisms for gene expression. The mechanisms for the TLR-independent induction of this p47 GTPase are currently under investigation.

To date, TLR2, TLR4, and TLR9 have been implicated in the recognition of *T. cruzi*-derived components (6, 14–16). TLR2 recognizes GPI-anchored mucin-like proteins and the *T. cruzi*-released protein Tc52 (6, 46, 47), whereas TLR4 is responsible for the recognition of glycoinositolphospholipids (15). TLR9 is also involved in the recognition of the CpG motif present in *T. cruzi* DNA (14). Among these *T. cruzi*-derived components, glycoinositolphospholipids can activate the TRIF-dependent pathway to induce IFN-β via TLR4. It is also possible that currently unknown components are recognized by TLR4 or TLR3, both of which use the TRIF-dependent pathway. Identification of such components responsible for the induction of IFN-β would provide important insights toward understanding innate immune responses to *T. cruzi* infection.

Acknowledgments

We thank Y. Yamada and K. Takeda for technical assistance, and M. Kurata for secretarial assistance.

Disclosures

The authors have no financial conflict of interest.

References

1. Krettli, A. U., and Z. Brener. 1982. Resistance against *Trypanosoma cruzi* associated to anti-living trypomastigote antibodies. *J. Immunol.* 128: 2009–2012.
2. Rottenberg, M., R. L. Cardoni, R. Andersson, E. L. Segura, and A. Orn. 1988. Role of T helper/inducer cells as well as natural killer cells in resistance to *Trypanosoma cruzi* infection. *Scand. J. Immunol.* 28: 573–582.
3. Tarleton, R. L. 1990. Depletion of CD8$^+$ T cells increases susceptibility and reverses vaccine-induced immunity in mice infected with *Trypanosoma cruzi*. *J. Immunol.* 144: 717–724.
4. Aliberti, J. C., M. A. Cardoso, G. A. Martins, R. T. Gazzinelli, L. Q. Vieira, and J. S. Silva. 1996. Interleukin-12 mediates resistance to *Trypanosoma cruzi* in mice and is produced by murine macrophages in response to live trypomastigotes. *Infect. Immun.* 64: 1961–1967.
5. Camargo, M. M., I. C. Almeida, M. E. Pereira, M. A. Ferguson, L. R. Travassos, and R. T. Gazzinelli. 1997. Glycosylphosphatidylinositol-anchored mucin-like glycoproteins isolated from *Trypanosoma cruzi* trypomastigotes initiate the synthesis of proinflammatory cytokines by macrophages. *J. Immunol.* 158: 5890–5901.
6. Ouaissi, A., E. Guilvard, Y. Delneste, G. Caron, G. Magistrelli, N. Herbault, N. Thieblemont, and P. Jeannin. 2002. The *Trypanosoma cruzi* Tc52-released protein induces human dendritic cell maturation, signals via Toll-like receptor 2, and confers protection against lethal infection. *J. Immunol.* 168: 6366–6374.
7. Reed, S. G. 1988. In vivo administration of recombinant IFN-γ induces macrophage activation, and prevents acute disease, immune suppression, and death in experimental *Trypanosoma cruzi* infections. *J. Immunol.* 140: 4342–4347.
8. Silva, J. S., P. J. Morrissey, K. H. Grabstein, K. M. Mohler, D. Anderson, and S. G. Reed. 1992. Interleukin 10 and interferon γ regulation of experimental *Trypanosoma cruzi* infection. *J. Exp. Med.* 175: 169–174.
9. Sonnenfeld, G., and F. Kierszenbaum. 1981. Increased serum levels of an interferon-like activity during the acute period of experimental infection with different strains of *Trypanosoma cruzi*. *Am. J. Trop. Med. Hyg.* 30: 1189–1191.
10. Kierszenbaum, F., and G. Sonnenfeld. 1982. Characterization of the antiviral activity produced during *Trypanosoma cruzi* infection and protective effects of exogenous interferon against experimental Chagas' disease. *J. Parasitol.* 68: 194–198.
11. Bogdan, C., J. Mattner, and U. Schleicher. 2004. The role of type I interferons in non-viral infections. *Immunol. Rev.* 202: 33–48.
12. Takeda, K., T. Kaisho, and S. Akira. 2003. Toll-like receptors. *Annu. Rev. Immunol.* 21: 335–376.
13. Akira, S., and K. Takeda. 2004. Toll-like receptor signalling. *Nat. Rev. Immunol.* 4: 499–511.
14. Shoda, L. K., K. A. Kegerreis, C. E. Suarez, I. Roditi, R. S. Corral, G. M. Bertot, J. Norimine, and W. C. Brown. 2001. DNA from protozoan parasites *Babesia bovis*, *Trypanosoma cruzi*, and *T. brucei* is mitogenic for B lymphocytes and stimulates macrophage expression of interleukin-12, tumor necrosis factor α, and nitric oxide. *Infect. Immun.* 69: 2162–2171.
15. Oliveira, A.-C., J. R. Peixoto, L. B. de Arruda, M. A. Campos, R. T. Gazzinelli, D. T. Golenbock, S. Akira, J. O. Previato, L. Mendonça-Previato, A. Nobrega, and M. Bellio. 2004. Expression of functional TLR4 confers proinflammatory responsiveness to *Trypanosoma cruzi* glycoinositolphospholipids and higher resistance to infection with *T. cruzi*. *J. Immunol.* 173: 5688–5696.
16. Petersen, C. A., K. A. Krumholz, and B. A. Burleigh. 2005. Toll-like receptor 2 regulates interleukin-1β-dependent cardiomyocyte hypertrophy triggered by *Trypanosoma cruzi*. *Infect. Immun.* 73: 6974–6980.
17. Campos, M. A., M. Closel, E. P. Valente, J. E. Cardoso, S. Akira, J. I. Alvarez-Leite, C. Ropert, and R. T. Gazzinelli. 2004. Impaired production of proinflammatory cytokines and host resistance to acute infection with *Trypanosoma cruzi* in mice lacking functional myeloid differentiation factor 88. *J. Immunol.* 172: 1711–1718.

18. Adachi, O., T. Kawai, K. Takeda, M. Matsumoto, H. Tsutsui, M. Sakagami, K. Nakanishi, and S. Akira. 1998. Targeted disruption of the MyD88 gene results in loss of IL-1- and IL-18-mediated function. *Immunity* 9: 143–150.
19. Yamamoto, M., S. Sato, H. Hemmi, K. Hoshino, T. Kaisho, H. Sanjo, O. Takeuchi, M. Sugiyama, M. Okabe, K. Takeda, and S. Akira. 2003. Role of adaptor TRIF in the MyD88-independent Toll-like receptor signaling pathway. *Science* 301: 640–643.
20. Müller, U., U. Steinhoff, L. F. Reis, S. Hemmi, J. Pavlovic, R. M. Zinkernagel, and M. Aguet. 1994. Functional role of type I and type II interferons in antiviral defense. *Science* 264: 1918–1921.
21. Taliaferro, W. H., and T. Pizzi. 1955. Connective tissue reactions in normal and immunized mice to a reticulotropic strain of *Trypanosoma cruzi*. *J. Infect. Dis.* 96: 199–226.
22. Vespa, G. N., F. Q. Cunha, and J. S. Silva. 1994. Nitric oxide is involved in control of *Trypanosoma cruzi*-induced parasitemia and directly kills the parasite in vitro. *Infect. Immun.* 62: 5177–5182.
23. Saeftel, M., B. Fleischer, and A. Hoerauf. 2001. Stage-dependent role of nitric oxide in control of *Trypanosoma cruzi* infection. *Infect. Immun.* 69: 2252–2259.
24. Silva, J. S., G. N. Vespa, M. A. Cardoso, J. C. Aliberti, and F. Q. Cunha. 1995. Tumor necrosis factor α mediates resistance to *Trypanosoma cruzi* infection in mice by inducing nitric oxide production in infected γ interferon-activated macrophages. *Infect. Immun.* 63: 4862–4867.
25. Castaños-Velez, E., S. Maerlan, L. M. Osorio, F. Åberg, P. Biberfeld, A. Örn, and M. E. Rottenberg. 1998. *Trypanosoma cruzi* infection in tumor necrosis factor receptor p55-deficient mice. *Infect. Immun.* 66: 2960–2968.
26. Ortiz-Ortiz, L., T. Ortega, R. Capin, and T. Martinez. 1976. Enhanced mononuclear phagocytic activity during *Trypanosoma cruzi* infection in mice. *Int. Arch. Allergy Appl. Immunol.* 50: 232–242.
27. Taylor, G. A., C. G. Feng, and A. Sher. 2004. p47 GTPases: regulators of immunity to intracellular pathogens. *Nat. Rev. Immunol.* 4: 100–109.
28. MacMicking, J. D. 2005. Immune control of phagosomal bacteria by p47 GTPases. *Curr. Opin. Microbiol.* 8: 74–82.
29. de Souza, A. P., B. Tang, H. B. Tanowitz, S. M. Factor, V. Shtutin, J. Shirani, G. A. Taylor, L. M. Weiss, and L. A. Jelicks. 2003. Absence of interferon-γ-inducible gene IGTP does not significantly alter the development of chagasic cardiomyopathy in mice infected with *Trypanosoma cruzi* (Brazil strain). *J. Parasitol.* 89: 1237–1239.
30. Isaacs, A., and J. Lindenmann. 1957. Virus interference. I. The interferon. *Proc. R. Soc. Lond. B. Biol. Sci.* 147: 258–267.
31. Decker, T., M. Müller, and S. Stockinger. 2005. The Yin and Yang of type I interferon activity in bacterial infection. *Nat. Rev. Immunol.* 5: 675–687.
32. Hess, C. B., D. W. Niesel, Y. J. Cho, and G. R. Klimpel. 1987. Bacterial invasion of fibroblasts induces interferon production. *J. Immunol.* 138: 3949–3953.
33. Niesel, D. W., C. B. Hess, Y. J. Cho, K. D. Klimpel, and G. R. Klimpel. 1986. Natural and recombinant interferons inhibit epithelial cell invasion by Shigella spp. *Infect. Immun.* 52: 828–833.
34. O'Connell, R. M., S. K. Saha, S. A. Vaidya, K. W. Bruhn, G. A. Miranda, B. Zarnegar, A. K. Perry, B. O. Nguyen, T. F. Lane, T. Taniguchi, et al. 2004. Type I interferon production enhances susceptibility to *Listeria monocytogenes* infection. *J. Exp. Med.* 200: 437–445.
35. Carrero, J. A., B. Calderon, and E. R. Unanue. 2004. Type I interferon sensitizes lymphocytes to apoptosis and reduces resistance to *Listeria* infection. *J. Exp. Med.* 200: 535–540.
36. Auerbuch, V., D. G. Brockstedt, N. Meyer-Morse, M. O'Riordan, and D. A. Portnoy. 2004. Mice lacking the type I interferon receptor are resistant to *Listeria monocytogenes*. *J. Exp. Med.* 200: 527–533.
37. Diefenbach, A., H. Schindler, N. Donhauser, E. Lorenz, T. Laskay, J. MacMicking, M. Rollinghoff, I. Gresser, and C. Bogdan. 1998. Type 1 interferon (IFNα/β) and type 2 nitric oxide synthase regulate the innate immune response to a protozoan parasite. *Immunity* 8: 77–87.
38. Mattner, J., A. Wandersee-Steinhauser, A. Pahl, M. Rollinghoff, G. R. Majeau, P. S. Hochman, and C. Bogdan. 2004. Protection against progressive leishmaniasis by IFN-β. *J. Immunol.* 172: 7574–7582.
39. Une, C., J. Andersson, and A. Orn. 2003. Role of IFN-α/β and IL-12 in the activation of natural killer cells and interferon-γ production during experimental infection with *Trypanosoma cruzi*. *Clin. Exp. Immunol.* 134: 195–201.
40. Taylor, G. A., C. M. Collazo, G. S. Yap, K. Nguyen, T. A. Gregorio, L. S. Taylor, B. Eagleson, L. Secrest, E. A. Southon, S. W. Reid, et al. 2000. Pathogen-specific loss of host resistance in mice lacking the IFN-γ-inducible gene IGTP. *Proc. Natl. Acad. Sci. USA* 97: 751–755.
41. Collazo, C. M., G. S. Yap, G. D. Sempowski, K. C. Lusby, L. Tessarollo, G. F. Woude, A. Sher, and G. A. Taylor. 2001. Inactivation of LRG-47 and IRG-47 reveals a family of interferon γ-inducible genes with essential, pathogen-specific roles in resistance to infection. *J. Exp. Med.* 194: 181–188.
42. Santiago, H. C., C. G. Feng, A. Bafica, E. Roffe, R. M. Arantes, A. Cheever, G. Taylor, L. Q. Vierira, J. Aliberti, R. T. Gazzinelli, and A. Sher. 2005. Mice deficient in LRG-47 display enhanced susceptibility to *Trypanosoma cruzi* infection associated with defective hemopoiesis and intracellular control of parasite growth. *J. Immunol.* 175: 8165–8172.
43. Stetson, D. B., and R. Medzhitov. 2006. Recognition of cytosolic DNA activates an IRF3-dependent innate immune response. *Immunity* 24: 93–103.
44. Andrade, L. O., and N. W. Andrews. 2004. Lysosomal fusion is essential for the retention of *Trypanosoma cruzi* inside host cells. *J. Exp. Med.* 200: 1135–1143.
45. Ishii, K. J., C. Coban, H. Kato, K. Takahashi, Y. Torii, F. Takeshita, H. Ludwig, G. Sutter, K. Suzuki, H. Hemmi, et al. 2006. A Toll-like receptor-independent antiviral response induced by double-stranded B-form DNA. *Nat. Immunol.* 7: 40–48.
46. Campos, M. A., I. C. Almeida, O. Takeuchi, S. Akira, E. P. Valente, D. O. Procopio, L. R. Travassos, J. A. Smith, D. T. Golenbock, and R. T. Gazzinelli. 2001. Activation of Toll-like receptor-2 by glycosylphosphatidylinositol anchors from a protozoan parasite. *J. Immunol.* 167: 416–423.
47. Ropert, C., I. C. Almeida, M. Closel, L. R. Travassos, M. A. Ferguson, P. Cohen, and R. T. Gazzinelli. 2001. Requirement of mitogen-activated protein kinases and IκB phosphorylation for induction of proinflammatory cytokines synthesis by macrophages indicates functional similarity of receptors triggered by glycosylphosphatidylinositol anchors from parasitic protozoa and bacterial lipopolysaccharide. *J. Immunol.* 166: 3423–3431.

Available online at www.sciencedirect.com
SCIENCE DIRECT®
Microbes and Infection 8 (2006) 1045–1053
Microbes and Infection
www.elsevier.com/locate/micinf

Original article

The involvement of immunoproteasomes in induction of MHC class I-restricted immunity targeting *Toxoplasma* SAG1

Kazunari Ishii [a], Hajime Hisaeda [a], Xuefeng Duan [a], Takashi Imai [a], Tohru Sakai [b], Hans Jörg Fehling [c], Shigeo Murata [d], Tomoki Chiba [d], Keiji Tanaka [d], Shinjiro Hamano [a], Miyuki Sano [a], Akihiko Yano [e], Kunisuke Himeno [a,*]

[a] *Department of Parasitology, Graduate School of Medical Sciences, Kyushu University, 3-1-1 Maidashi, Higashi-ku, Fukuoka 812-8582, Japan*
[b] *Department of Nutrition, Osaka Prefecture College of Nursing, Osaka 583-8555, Japan*
[c] *Department of Immunology, University of Ulm, 89070 Ulm, Germany*
[d] *Department of Molecular Oncology, The Tokyo Metropolitan Institute of Medical Science, Tokyo 113-8613, Japan*
[e] *Department of Infection and Host Defense, Graduate School of Medicine, Chiba University, Chiba 260-8672, Japan*

Received 21 July 2005; accepted 25 October 2005
Available online 18 January 2006

Abstract

The ubiquitin–proteasome system (UPS) plays an indispensable role in inducing MHC class I-restricted $CD8^+$ T cells and was exploited in the development of a DNA vaccine against the intracellular protozoan *Toxoplasma gondii* by constructing a chimeric DNA encoding a fusion protein between murine ubiquitin and the toxoplasma antigen SAG1. The SAG1 peptide was promptly degraded in antigen-presenting cells (APCs) transfected with the chimeric DNA. Degradation, however, was hampered by incubating the APCs with the proteasome inhibitor epoxomicin. Mice vaccinated with the DNA acquired potent protective immunity mediated by MHC class I-restricted $CD8^+$ T cells against infection by the highly virulent *Toxoplasma*. The accelerated degradation and induction of immunity were dependent on the UPS since mice lacking an immuno-subunit of 20S proteasome, LMP7, lost these functions, although they were independent of the proteasome regulator PA28α/β complex.

Keywords: Antigen presentation/processing; Vaccination; Parasitic-protozoan; CTL

1. Introduction

Classical $CD8^+$ T cells recognize antigens presented to MHC class I molecules on APCs. Endogenous antigenic proteins such as oncogene products and viral products synthesized within the APC are first polyubiquitinated and then degraded into their peptide components by the proteasome. This type of antigen processing system has been generally accepted as the ubiquitin–proteasome system (UPS) [1–3]. These peptides are subsequently transported into the endoplasmic reticulum through the transporter associated with antigen processing (TAP) and then loaded onto MHC class I molecules. Once the antigenic peptides have bound to MHC class I molecules, the peptide/MHC class I complexes are transported to the surface of the APC via the Golgi system and then the peptides are presented to T cell receptors of $CD8^+$ T cells.

Infections with intracellular pathogens such as *Mycobacterium tuberculosis*, *Toxoplasma gondii* and *Cytomegalovirus* have attracted much attention in clinical fields because of resistance to chemotherapy and/or the lack of effective vaccines [4]. Cellular immunity, especially $CD8^+$ T cell responses, plays essential roles in the protection against such pathogens, while humoral immunity has a negligible effect [5]. However, conventional vaccine strategies using microbial proteins/peptides or DNA have often failed to induce a protective immune

Abbreviations: APC, antigen-presenting cell; CTL, cytotoxic T cell; UPS, ubiquitin–proteasome system; UFD, ubiquitin-fusion degradation pathway.

* Corresponding author. Tel.: +81 92 642 6116; fax: +81 92 642 6115.
E-mail address: himeno@parasite.med.kyushu-u.ac.jp (K. Himeno).

1286-4579/$ - see front matter © 2005 Elsevier SAS. All rights reserved.
doi:10.1016/j.micinf.2005.10.023

response involving $CD8^+$ T cells [1–3]. Therefore, new vaccine strategies are urgently needed.

The intracellular protozoan *T. gondii* is a major opportunistic pathogen in immunocompromised patients worldwide. Among the proposed vaccine candidates, the SAG1 protein is the most well characterized. This 30-kDa protein is the major surface antigen of *T. gondii* tachyzoites [6] and is highly conserved in *T. gondii* strains [7]. It induces high antibody levels in humans and has been identified in all the serum samples from infected subjects [8]. $CD8^+$ cytotoxic T cells (CTLs) play an essential role in protection against a highly virulent RH strain of *T. gondii* [9]. Some $CD8^+$ CTL epitopes included in SAG1 have been identified [10]. Nevertheless, most vaccine trials, including trials using DNA vaccines have resulted in failure to prevent infection by the highly virulent RH strain [11], although vaccination with cultured and attenuated *Toxoplasma* is effective [10,12].

In the present study, we developed a new strategy for vaccination against highly virulent *T. gondii* employing a chimeric DNA encoding SAG1 fused with ubiquitin at its N-terminus. The gene product is expected to be processed by the ubiquitin-fusion degradation pathway (UFD), a virtual route of the UPS [13], and then routed to the MHC class I molecules, resulting in the activation of SAG1-specific $CD8^+$ T cells. The crucial role of the UPS was demonstrated by using the proteasome inhibitor epoxomicin and immunoproteasome subunit LMP7-deficient mice. Further, dependency of this type of vaccination on the proteasome regulator PA28 was examined by employing PA28-deficient mice.

2. Materials and methods

2.1. Animals and parasites

We performed mouse studies in accordance with the institutional guidelines of Kyushu University. Female 7-week-old BALB/c ($H\text{-}2^d$) and C57BL/6 (B6, $H\text{-}2^b$) mice were purchased from Seac Yoshitomi, Ltd. (Fukuoka, Japan). B6.LMP7-deficient mice [14] and B6.PA28α/β-deficient mice [15] established by us were used in experiments. A highly virulent RH strain of *T. gondii* [16,17] was used in this study. The parasites were maintained by serial passages in ddY mice. Tachyzoites were isolated for infection as previously described [18,19].

2.2. Plasmids

The gene encoding SAG1 (aa 61–286) was amplified by PCR from *T. gondii* genomic DNA from the RH strain using a forward and reverse primer pair. The gene encoding mouse ubiquitin (aa 1–76) with mutation 76G→A was amplified by PCR from genomic DNA obtained from livers of B6 mice. The PCR products were subcloned into pGEM-T (Promega, Madison, WI) and their DNA sequences were confirmed by the dideoxy-mediated chain termination method.

DNA fragments encoding SAG1 or ubiquitin excised from the pGEM-T plasmids were cloned into the *Eco*RI and *Bam*HI sites of a pcDNA3.1 vector (Invitrogen, Carlsbad, CA), and designated pcDNA-SAG1 or pcDNA-UB, respectively. To fuse DNA encoding SAG1 to that encoding ubiquitin, a SAG1 gene fragment from the pGEM-T plasmid was introduced into the *Hind*III and blunted *Afl*II sites of the pcDNA-UB vector, designated pcDNAUB-SAG1. pcDNA3.1 is a mammalian expression plasmid containing a CMV promoter and bovine growth hormone poly A sequences. These plasmids were replicated in *Escherichia coli* DH5α and prepared using an endotoxin-free plasmid preparation kit (Invitrogen).

2.3. DNA vaccination

For vaccination, a gene gun (Bio-Rad, Hercules, CA) was used as previously described [20]. Briefly, plasmid DNA was precipitated onto 1.6 μg of gold particles and coated onto the inner surface of tubing by a tube loader. The final tubing segment resulted in delivery of 0.125 mg of gold particles and 2 μg of plasmid DNA per transfection. pcDNA-SAG1 (native form) and pcDNAUB-SAG1 (ubiquitin-fusion form) were transferred to three different portions of shaved abdominal skin four times at 2-week intervals. A total of 24 μg of plasmid was administered to each mouse.

2.4. RT-PCR

Total RNA was purified from draining lymph nodes using a total RNA isolation reagent (Invitrogen) 48 h after the last immunization. Single-strand cDNA was synthesized from 2 μg of total RNA by using reverse transcriptase (Invitrogen). Genes encoding SAG1 and β-actin as an internal control were amplified by PCR from the cDNA with the sense and antisense primer pairs 5′-CAGCACTCTTGGTCCTGTCA-3′, 5′-GCACCCTTATCACTCGAAGC-3′ for SAG1 and 5′-TGG AATCCTGTGGCATCCATGAAAC-3′, 5′-TAAACGCAGCT CAGTAACAGTCCG-3′ for β-actin. The expected size of the PCR product from SAG1 was 210 bp and from β-actin was 348 bp.

2.5. Transfection and immunoblotting

COS-7 cells were transfected with the SAG1-expressing plasmids by using lipofection reagent (Invitrogen) and cultured for 24 h. In some experiments, transfected cells were cultured with epoxomicin (Peptide Institute, Inc., Japan). Cell lysates and supernatants were separated by SDS-PAGE and transferred onto PVDF filters. Proteins bound to the filter were detected with mice anti-SAG1 sera and HRP-conjugated polyclonal antibodies to mouse IgG (Zymed, San Francisco, CA) and visualized on X-ray film by chemiluminescent Western blotting detection (Amersham Pharmacia Biotech, UK) method. The expression of SAG1 was quantified by densitometric analysis (Fuji Photo Film Co., Ltd., Japan).

2.6. Cell purification and culture

$CD8^+$ T cells were purified from mice spleen cells using Magnetic Separation Columns (Miltenyi Biotec, Germany)